INTERNATIONAL JOURNAL FOR NUMERICAL METHODS IN ENGINEERING
Int. J. Numer. Meth. Engng 2009; **80**:163–190
Published online 23 April 2009 in Wiley InterScience (www.interscience.wiley.com). DOI: 10.1002/nme.2624

Subdomain radial basis collocation method for heterogeneous media

Jiun-Shyan Chen[1,*,†,‡], Lihua Wang[2,§], Hsin-Yun Hu[3,¶] and Sheng-Wei Chi[1,‖]

[1]*Civil and Environmental Engineering Department, University of California Los Angeles (UCLA), Los Angeles, CA 90095, U.S.A.*
[2]*School of Aerospace Engineering and Applied Mechanics, Tongji University, Shanghai, People's Republic of China*
[3]*Mathematics Department, Tunghai University, Taichung, Taiwan*

SUMMARY

Strong form collocation in conjunction with radial basis approximation functions offer implementation simplicity and exponential convergence in solving partial differential equations. However, the smoothness and nonlocality of radial basis functions pose considerable difficulties in solving problems with local features and heterogeneity. In this work, we propose a simple subdomain strong form collocation method, in which the approximation in each subdomain is constructed separately. Proper interface conditions are then imposed on the interface. Under the subdomain strong form collocation construction, it is shown that both Neumann and Dirichlet boundary conditions should be imposed on the interface to achieve the optimum convergence. Error analysis and numerical tests consistently confirm the need to impose the optimal interface conditions. The performance of the proposed methods in dealing with heterogeneous media is also validated. Copyright © 2009 John Wiley & Sons, Ltd.

Received 24 October 2008; Revised 25 February 2009; Accepted 26 February 2009

KEY WORDS: radial basis functions; collocation method; subdomain collocation; meshfree method; heterogeneous media

*Correspondence to: Jiun-Shyan Chen, Civil and Environmental Engineering Department, University of California Los Angeles, Los Angeles, CA 90095, U.S.A.
†E-mail: jschen@seas.ucla.edu
‡Professor.
§Graduate student and visiting student.
¶Assistant Professor.
‖Graduate student.

Contract/grant sponsor: Lawrence Livermore National Laboratory (U.S.A.)
Contract/grant sponsor: National Natural Science Foundation of China (NSFC); contract/grant number: 10572104
Contract/grant sponsor: National Science Council of Taiwan; contract/grant number: NSC 96-2115-M-029-002-MY2

1. INTRODUCTION

In recent years, development of meshfree methods offers new dimensions for solving partial differential equations (PDE). Meshfree methods can be classified into two types, one based on Galerkin weak form integrated by quadrature rules [1–6] and the other based on strong form with direct collocation [7–12]. Galerkin formulation yields a symmetric discrete equation and allows lower continuity in the test and trial functions, but the need of quadrature rules for domain integration and special treatment of Dirichlet boundary conditions adds considerable complexity and computational cost. Methods based on strong form, such as radial basis collocation method (RBCM), on the other hand, avoid quadrature rules and simplifies imposition of boundary conditions, but the nonlocality of the radial basis functions (RBF) renders full matrix and ill-conditioning in the discrete system. The smooth approximation and nonlocality in the RBFs also cause obstruction in solving problems with heterogeneous media.

Several methods have been proposed to deal with ill-conditioned discrete equations in the RBCM. Much effort has been devoted to localize the RBFs. Schaback and Wendland [13] and Wendland [14, 15] introduced a class of positive definite and compactly supported RBFs, which consist of a univariate polynomial within their support. The accuracy of the approach can be improved by using a large scaling factor but is costly. Xiao and McCarthy [16] presented a local-weighted residual method with the Heaviside step function as the weighting function over a local domain, and with the RBF as the trial function. Wang and Liu [17] introduced an influence domain to the RBF approximation where each influence domain is localized. In this work, an approach similar to a transformation method [5, 18] was also introduced to obtain the interpolation properties. A local weak form with RBF approximation was proposed by Liu and Gu [19] to yield a sparse discrete system. Shu *et al.* [20] introduced RBFs in the direct collocation of PDE by computing derivatives based on a differential quadrature scheme within a local domain of influence. Chen *et al.* [21] proposed a reproducing kernel (RK) enhanced RBF approximation to achieve a local approximation, which holds the similar convergence property as that of the RBF collocation method while yielding a banded and better-conditioned discrete system. Methods have also been introduced to remedy ill-conditioning problem. The block partitioning method by Wong *et al.* [22] and Kansa and Hon [23] takes the advantage of better conditioning of each sub-block. Fasshauer [8] investigated global and local RBFs and introduced smoothing methods and multilevel algorithm for enhancement of ill-conditioning. An adaptive algorithm [24] has been proposed to properly select suitable test and trial spaces iteratively.

Despite of the tremendous advancement in the RBCM, little has been done in addressing solvability of problems with heterogeneity and material interfaces using this class of methods. Two major difficulties exist in applying RBCM to heterogeneous media. One is due to the nonlocality of the RBF, where the local characters cannot be precisely represented by the nonlocal approximation. The other is the difficulty of approximating derivative discontinuity across the material interface by the smooth RBF. We note that the treatment of derivative discontinuity in the arena of 'meshfree methods' has been extensively investigated due to the use of smooth moving least squares (MLS) or RK functions as the test and trial functions in solving PDEs, but these approaches, such as Lagrange multiplier method [25] and interface enrichment techniques [26, 27], have been applied to weak form type framework with local test and trial functions.

In this work, we focus on the treatment of derivative discontinuity under strong form collocation with RBF type of approximation, and present a subdomain RBCM to resolve the above-mentioned difficulties. We first perform partitioning of the total domain and define subdomains according to

DOI: 10.1002/nme

heterogeneity of the problem. The solution of each subdomain is approximated only by the RBFs with source points located in the domain and on the boundaries of the subdomain. The strong form of the original problem is first imposed at the collocation points in each subdomain using the RBFs in the same subdomain in such a way that they are treated as separate subdomain problems. The solution of the total domain is then obtained by gluing the solution along the interfaces of the subdomains by imposing interface conditions with direct collocation. These interface conditions and the direct collocation of strong form and the associated boundary conditions are then solved simultaneously to obtain the overall solution of the original problem. The critical consideration in this approach is the type of interface conditions to be imposed. For elasticity problems, we show that imposition of both displacement continuity conditions and traction continuity conditions yields the best results. This has been identified by error analysis and numerical examples presented in this paper. We also demonstrate that for problems with localized behavior near material interfaces, localized RBFs (L-RBFs) are needed in addition to the subdomain treatment. A L-RBF constructed under the partition of unity framework [21] is employed for this purpose in this work.

The formulation and implementation algorithms of the proposed methods presented in this paper are organized as follows. We first give an overview of RBFs and L-RBFs constructed under partition of unity in Section 2. In Section 3, we first show numerically and analytically why strong form approach does not converge for heterogeneous materials, and followed by presentation of a subdomain approximation for the solution of PDE with heterogeneous material constants. The imposition of interface condition in a strong form and implementation details are also described in this section. In Section 4, we provide error analysis of subdomain collocation method with a special attention devoted to the imposition of interface conditions. We conclude that both displacement continuity and traction equilibrium are required on the interfaces for optimum solution accuracy. Several numerical examples are given in Section 5 to validate the adequacy of the interface conditions and to examine the accuracy and convergence of the proposed subdomain collocation method. Conclusions are given in Section 6.

2. APPROXIMATION FUNCTIONS

2.1. Radial basis functions

RBFs were originally constructed for interpolation by Hardy [28], and have received much attention in recent years in solving PDE's due to the seminal work of Kansa [7, 12]. We take a commonly used multiquadrics RBFs as an example

$$g_I(\mathbf{x}) = (r_I^2 + c^2)^{n-(3/2)}, \quad n = 1, 2, 3, \ldots \tag{1}$$

where $r_I = \|\mathbf{x} - \mathbf{x}_I\|$, the point $\mathbf{x}_I$ is called the source point, and the constant c involved in Equation (1) is called the shape parameter of RBFs. The approximation of a function $u(\mathbf{x})$ in Ω discretized by a set of N_s source points $\mathbf{S}$, $\mathbf{S} = [\mathbf{x}_1, \mathbf{x}_2, \ldots, \mathbf{x}_{N_s}] \subseteq \Omega \cup \partial\Omega$ is expressed as

$$u^h(\mathbf{x}) = \sum_{I=1}^{N_s} g_I(\mathbf{x}) a_I + p(\mathbf{x}) \tag{2}$$

where a_I is the expansion coefficient, $p(\mathbf{x}) \in P_t$ is polynomial of degree less than t, and $g_I(\mathbf{x})$ is the RBF.

DOI: 10.1002/nme

Remark 2.1

1. RBFs are global nonlocal functions. The intensity (not locality) of the functions is controlled by the shape parameter c; smaller c yields more concentrated function near source point $\mathbf{x}_I$. In RBFs approximation, the shape parameter has profound influence on the accuracy and convergence of the approximation.
2. RBFs alone do not have polynomial reproducibility. The polynomial function $p(\mathbf{x})$ in (2) is used to achieve polynomial reproducibility.
3. RBFs are infinitely continuous differentiable (C^∞). This allows the solution of PDE with RBFs approximation be accomplished by a direct strong form collocation called the RBCM. However, due to the nonlocal character of RBFs, the resulting discrete equations associated with PDE are full matrices and often ill-conditioned as the discretization is refined.
4. To achieve optimum solution in RBCM, more collocation points than sources points should be used and thus yields an over-determined system. For solving the over-determined system, one may use QR decomposition, singular value decomposition (SVD), or Cholesky decomposition on its normal equation. These procedures are typically more expensive than that of the finite element methods (FEMs).
5. If certain regularity conditions of the approximated function u and the RBFs g_I are met, RBFs approximation possesses the following exponential convergence property [29]

$$\|u-u^h\|_{L^\infty(\Omega)} \leqslant C\eta^{c/h}\|u\|_t \tag{3}$$

where C is a constant independent of c and h, $0<\eta<1$ is a real number, and $\|\cdot\|_t$ is induced form defined in [29].

2.2. *Localized radial basis functions*

L-RBFs have been proposed to yield banded discrete differential operator and to reduce ill-conditioning of the matrix. We consider the following L-RBFs constructed under partition of unity framework [21]

$$u^h(\mathbf{x}) = \sum_{I=1}^{N} [\phi_I(\mathbf{x})(a_I + g_I(\mathbf{x})d_I)] \tag{4}$$

where $\phi_I(\mathbf{x})$ is a partition of unity localizing function with compact support that has polynomial reproducibility, that is

$$\sum_I \phi_I(\mathbf{x})\mathbf{x}_I^\alpha = x^\alpha, \quad |\alpha| \leqslant p \tag{5}$$

where $\mathbf{x}^\alpha = x_1^{\alpha_1}\dots x_d^{\alpha_d}$, and $|\alpha| = \sum_{i=1}^d \alpha_i$, and p is the order of that can be exactly reproduced. The partition of unity function $\phi_I(\mathbf{x})$ with compact support can be constructed with MLS [1, 30] or RK approximation [2].

Remark 2.2

1. In two-dimensional elasticity solved by strong form collocation, the bounds in condition numbers using multiquadrics RBF, the RK function $\phi_I(\mathbf{x})$ that has compact support, and L-RBF of Equation (4) constructed using RK function $\phi_I(\mathbf{x})$ as localizing function of RBF are compared below [21]

DOI: 10.1002/nme

RBF: Cond. $\approx O(h^{-8})$
RK: Cond. $\approx O(h^{-2})$
L-RBF: Cond. $\approx O(h^{-3})$

where h is the nodal distance. In this estimate, the support of the RK function $\phi_I(\mathbf{x})$ is selected to be the minimum allowable support so that the polynomial reproducibility in (5) holds [5]. It is shown above that the condition number of L-RBFs in (4) following [21] is much smaller than the standard global RBFs and only slightly larger than the local partition of unity function such as the RK function.

2. The error analysis [21] shows that if the error of RK approximation in (4) is sufficiently small, solving PDE by strong form collocation with L-RBFs approximation maintains the exponential convergence of RBFs, as opposed to the algebraic convergence rate in standard RK approximation, while significantly improving the conditioning of the discrete system and yielding a banded matrix.
3. The total operation count for solving PDE with L-RBFs collocation method has been discussed in [21].
4. In this work, we focus on how to deal with discontinuous derivatives when standard nonlocal RBFs are employed as approximation functions. We will only introduce the L-RBFs when fine features exist in the problem, such as the existence of boundary layers as demonstrated in the numerical examples.

3. SUBDOMAIN RBCM FOR HETEROGENEOUS ELASTICITY

3.1. Difficulty in RBCM for heterogeneous elasticity

The smooth and nonlocal nature of RBFs renders difficulty in PDE with heterogeneous coefficients. Consider a one-dimensional elasticity without body force

$$\begin{gathered}\frac{\mathrm{d}}{\mathrm{d}x}\left(E(x)\frac{\mathrm{d}u}{\mathrm{d}x}\right)=0, \quad x\in(0,10)\\ u(0)=0, \quad u(10)=1\end{gathered} \tag{6}$$

with heterogeneous Young's modulus

$$E(x)=\begin{cases}E^+, & x\in[0,5]\\ E^-, & x\in(5,10]\end{cases} \tag{7}$$

where $E^+=10^3$, $E^-=10^4$. Let u^h be the approximation of the unknown u by RBFs

$$u^h(x)=\sum_{I=1}^{N_s} g_I(x)a_I \tag{8}$$

DOI: 10.1002/nme

where $g_I(x)$ is the one-dimensional nonlocal multiquadrics RBFs and N_s is the number of source points. We impose the strong form in (6) at N_c collocation points to yield the following discrete equation:

$$\begin{bmatrix} g_1(x_1) & \cdots & g_{N_s}(x_1) \\ E(x_2)g_{1,xx}(x_2) & \cdots & E(x_2)g_{N_s,xx}(x_2) \\ \vdots & & \vdots \\ E(x_{N_c-1})g_{1,xx}(x_{N_c-1}) & \cdots & E(x_{N_c-1})g_{N_s,xx}(x_{N_c-1}) \\ g_1(x_{N_c}) & \cdots & g_{N_s}(x_{N_c}) \end{bmatrix} \begin{bmatrix} a_1 \\ \vdots \\ a_{N_s} \end{bmatrix} = \begin{bmatrix} 0 \\ 0 \\ \vdots \\ 0 \\ 1 \end{bmatrix} \tag{9}$$

The first and last equations are associated with the two boundary conditions and the rest of N_c-2 equations refer to the strong form collocation of the differential equation. For sufficient accuracy, the number of collocation points N_c should be greater than the number of source points N_s. In this problem, we use $N_c=4N_s$, which yields the best accuracy. This over-determined system in (9) is solved by least-squares method. In the first test, we use shape parameter $c=5.0$ and uniform discretization with $N_s=41$, 81, and 161, and the numerical results in Figure 1(a) show essentially no convergence since the numerical model fails to capture the derivative discontinuity. We then reduce the shape parameter to $c=1.2$ to better capture the material interface as shown in Figure 1(b), but the method converges to a wrong solution.

By re-examining this problem and with the consideration of the discontinuous Young's modulus, the differential equation in Equation (6) is re-written as

$$E(x)u_{,xx}(x)+E_{,x}(x)u_{,x}(x)=0 \tag{10}$$

Since $E_{,x}(x)=\delta(x-5)$, Equation (10) is expressed as

$$E(x)u_{,xx}(x)+\delta(x-5)u_{,x}(x)=0 \tag{11}$$

Thus, the strong form collocation of (11) with boundary conditions in Equation (6) is

$$\left\{ \begin{bmatrix} g_1(x_1), & \ldots, & g_{N_s}(x_1) \\ E(x_2)g_{1,xx}(x_2), & \ldots, & E(x_2)g_{N_s,xx}(x_2) \\ \vdots & & \vdots \\ E(x_{N_c-1})g_{1,xx}(x_{N_c-1}), & \ldots, & E(x_{N_c-1})g_{N_s,xx}(x_{N_c-1}) \\ g_1(x_{N_c}), & \ldots, & g_{N_s}(x_{N_c}) \end{bmatrix} + \begin{bmatrix} 0, & \ldots, & 0 \\ \delta(x_2-5)g_{1,x}(x_2), & \ldots, & \delta(x_2-5)g_{N_s,x}(x_2) \\ \vdots & & \vdots \\ \delta(x_{N_c-1}-5)g_{1,x}(x_{N_c-1}), & \ldots, & \delta(x_{N_c-1}-5)g_{N_s,x}(x_{N_c-1}) \\ 0, & \ldots, & 0 \end{bmatrix} \right\} \begin{bmatrix} a_1 \\ \vdots \\ a_{N_s} \end{bmatrix} = \begin{bmatrix} 0 \\ 0 \\ \vdots \\ 0 \\ 1 \end{bmatrix} \tag{12}$$

DOI: 10.1002/nme

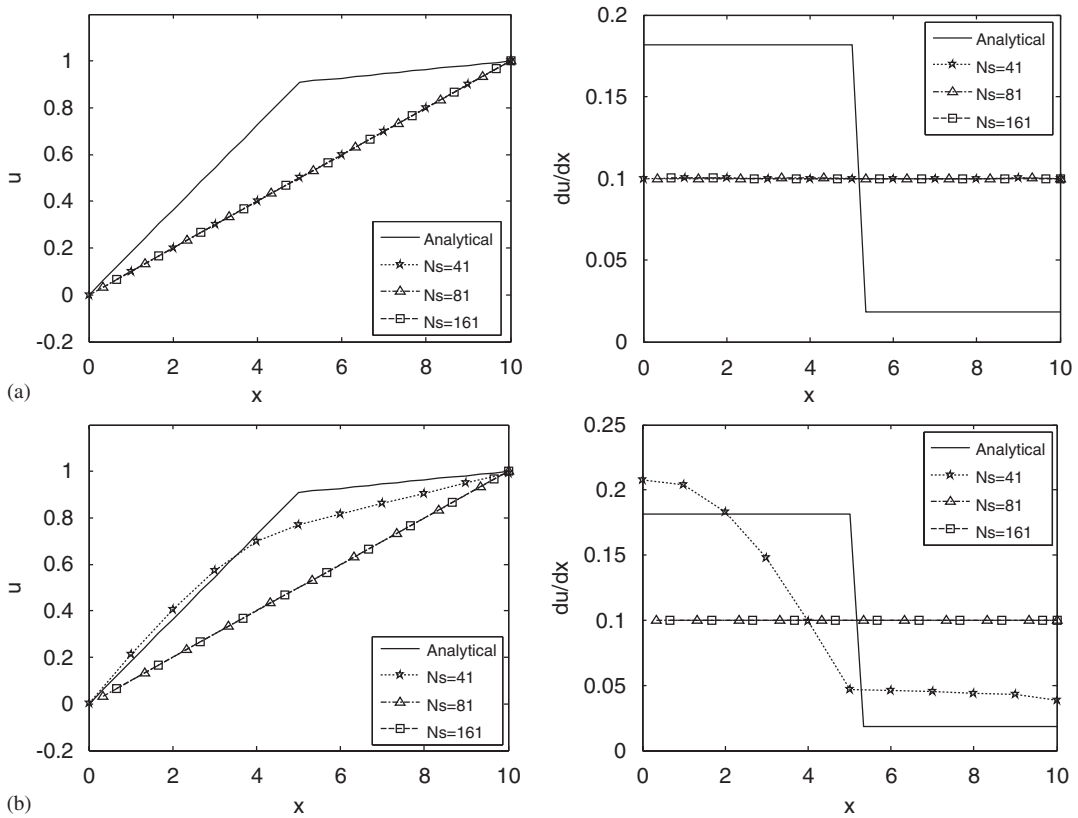

Figure 1. (a) Numerical solutions of a one-dimensional elastic composite using radial basis collocation method with large shape parameter $c=5.0$ and (b) numerical solutions of a one-dimensional elastic composite using radial basis collocation method with small shape parameter $c=1.2$.

It is clear that the term $\delta(x_J-5)g_{I,x}(x_J)$ is omitted in (9) unless one of the collocation points is exactly on the interface, and this yields the results in Figures 1(a)–(b) where the numerical solutions do not capture material interface and yield a straight line. On the other hand, having collocation points located on the interface yields singularity in $\delta(x_J-5)g_{I,x}(x_J)$, and Equation (9) cannot be solved directly unless the delta function is regularized. Thus, we propose the subdomain collocation method to alleviate this difficulty in the next section.

3.2. Basic equations

We first consider the original heterogeneous problem of the following form:

$$L^\tau u^\tau = f^\tau \quad \text{in } \Omega \tag{13}$$

$$B^\tau u^\tau = q^\tau \quad \text{on } \partial\Omega \tag{14}$$

where Ω is the open domain, $\partial\Omega$ is the boundary of Ω, L^τ is the differential operator in Ω, B^τ is the boundary operator defined on $\partial\Omega$, which contains both the Dirichlet and Neumann boundary

DOI: 10.1002/nme

operators, f^τ is the source term, q^τ is associated with boundary conditions, and the superscript τ denotes the heterogeneity of the problem. In most elasticity problems, the heterogeneity is resulting from heterogeneous elasticity constants in the differential operator or the heterogeneity of body force, but in some special cases heterogeneity could exist in boundary conditions. In this paper, we focus on material heterogeneity and that yields weak discontinuity (derivative discontinuity) in the solution.

For easy illustration we consider a domain composed of two materials, each occupies Ω^+ and Ω^- as shown in Figure 2. We denote by $\partial\Omega^+$ and $\partial\Omega^-$ the boundaries of Ω^+ and Ω^-, respectively, and closed domains $\bar{\Omega}=\Omega\cup\partial\Omega$, $\bar{\Omega}^+=\Omega^+\cup\partial\Omega^+$, $\bar{\Omega}^-=\Omega^-\cup\partial\Omega^-$, and we have $\bar{\Omega}=\bar{\Omega}^+\cup\bar{\Omega}^-$, $\Omega^+\cap\Omega^-=\emptyset$, and $\Gamma=\partial\Omega^+\cap\partial\Omega^-$ is the interface. In each subdomain, the material is homogeneous. We consider the transformation of the original problem to the following subdomain problem:

$$\begin{aligned} L^+u^+ &= f^+ \quad \text{in } \Omega^+ \\ B^+u^+ &= q^+ \quad \text{on } \partial\Omega^+\cap\partial\Omega \end{aligned} \tag{15}$$

$$\begin{aligned} L^-u^- &= f^- \quad \text{in } \Omega^- \\ B^-u^- &= q^- \quad \text{on } \partial\Omega^-\cap\partial\Omega \end{aligned} \tag{16}$$

$$I(u^+,u^-)=0 \quad \text{on } \Gamma \tag{17}$$

where I is the operator representing interface conditions on Γ, which plays a critical role on the accuracy and convergence of the proposed method. The solution of originally heterogeneous problem in (13)–(14) is now solved in each subdomain in (15) and (16), *separately*, with additional interface condition in (17) to 'glue' the two subdomain solutions together. We will give detailed discussion on the appropriate construction of I for heterogeneous elasticity in the next section. The solution in each subdomain is approximated by separate set of basis functions

$$u^h(\mathbf{x})=\begin{cases} u^{h+}(\mathbf{x})=g_1^+(\mathbf{x})a_1^+ +\cdots+g_{N_s^+}^+(\mathbf{x})a_{N_s^+}^+, & \mathbf{x}\in\bar{\Omega}^+ \\ u^{h-}(\mathbf{x})=g_1^-(\mathbf{x})a_1^- +\cdots+g_{N_s^-}^-(\mathbf{x})a_{N_s^-}^-, & \mathbf{x}\in\bar{\Omega}^- \end{cases} \tag{18}$$

where N_s^+ and N_s^- are the number of source points in the two subdomains, and $\{g_I^+\}_{I=1}^{N_s^+}$ and $\{g_I^-\}_{I=1}^{N_s^-}$ are two sets of RBFs with their corresponding source points $\{x_I^+\}_{I=1}^{N_s^+}$ and $\{x_I^-\}_{I=1}^{N_s^-}$ located in $\bar{\Omega}^+$ and $\bar{\Omega}^-$, respectively. The coefficients $\{a_I^+\}_{I=1}^{N_s^+}$ and $\{a_I^-\}_{I=1}^{N_s^-}$ are obtained by solving strong form collocation and interface conditions of Equations (15)–(17) simultaneously.

3.3. Subdomain collocation for heterogeneous elasticity

The strong form of an elasticity problem is given as follows:

$$(C_{ijkl}u_{(k,l)})_{,j}+b_i=0 \quad \text{in } \Omega \tag{19}$$

$$C_{ijkl}u_{(k,l)}n_j=h_i \quad \text{on } \partial\Omega_h \tag{20}$$

$$u_i=\bar{g}_i \quad \text{on } \partial\Omega_g \tag{21}$$

DOI: 10.1002/nme

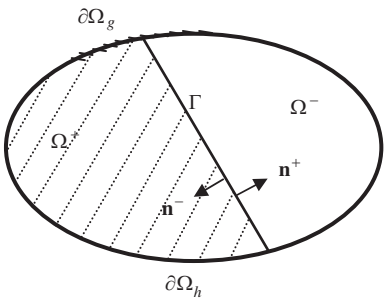

Figure 2. Two subdomains of a problem with material heterogeneity.

where C_{ijkl} is the elasticity tensor, u_i is the displacement, $(\cdot)_{,j} \equiv \partial(\cdot)/\partial x_j$, b_i is the body force, h_i is the surface traction on Neumann boundary $\partial\Omega_h$, g_i is the prescribed boundary displacement on Dirichlet boundary $\partial\Omega_g$, and $\partial\Omega = \partial\Omega_h \cup \partial\Omega_g$. For heterogeneous materials, C_{ijkl} is a function of position, and it yields nonsmooth solution if C_{ijkl} is discontinuous across material interfaces.

Based on the heterogeneity of C_{ijkl}, we decompose domain into n subdomains $\Omega = \bigcup_{i=1}^{n} \Omega^{(i)}$, $\Omega^{(i)} \cap \Omega^{(j)} = \emptyset$ if $i \neq j$, so that C_{ijkl} is a constant tensor in each subdomain. For simplicity we consider a domain composed of two materials. The corresponding sub-problems are expressed as:

$$\begin{aligned}
(C^+_{ijkl} u^+_{(k,l)})_{,j} + b^+_i &= 0 \quad \text{in } \Omega^+ \\
u^+_i &= \bar{g}^+_i \quad \text{on } \partial\Omega^+ \cap \partial\Omega_g \\
C^+_{ijkl} u^+_{(k,l)} n^+_j &= h^+_i \quad \text{on } \partial\Omega^+ \cap \partial\Omega_h
\end{aligned} \tag{22}$$

$$\begin{aligned}
(C^-_{ijkl} u^-_{(k,l)})_{,j} + b^-_i &= 0 \quad \text{in } \Omega^- \\
u^-_i &= \bar{g}^-_i \quad \text{on } \partial\Omega^- \cap \partial\Omega_g \\
C^-_{ijkl} u^-_{(k,l)} n^-_j &= h^-_i \quad \text{on } \partial\Omega^- \cap \partial\Omega_h
\end{aligned} \tag{23}$$

with the following interface conditions:

$$\begin{aligned}
u^+_i - u^-_i &= 0 \\
C^+_{ijkl} u^+_{(k,l)} n^+_j + C^-_{ijkl} u^-_{(k,l)} n^-_j &= 0
\end{aligned} \quad \text{on } \Gamma \tag{24}$$

Remark 3.1
For elasticity, we consider both displacement continuity and traction equilibrium on the interface. It will be shown in the next section that the imposition of both displacement continuity and traction equilibrium conditions yields the best convergence of this method.

For notational simplicity, Equations (22)–(24) are symbolically expressed as follows:

$$\begin{aligned}
\mathbf{L}^+ \mathbf{u}^+ &= \mathbf{f}^+ \quad \text{in } \Omega^+ \\
\mathbf{B}^+_g \mathbf{u}^+ &= \mathbf{g}^+ \quad \text{on } \partial\Omega^+ \cap \partial\Omega_g \\
\mathbf{B}^+_h \mathbf{u}^+ &= \mathbf{h}^+ \quad \text{on } \partial\Omega^+ \cap \partial\Omega_h
\end{aligned} \tag{25}$$

DOI: 10.1002/nme

$$\begin{aligned} \mathbf{L}^- \mathbf{u}^- &= \mathbf{f}^- \quad \text{in } \Omega^- \\ \mathbf{B}_g^- \mathbf{u}^- &= \mathbf{g}^- \quad \text{on } \partial\Omega^- \cap \partial\Omega_g \\ \mathbf{B}_h^- \mathbf{u}^- &= \mathbf{h}^- \quad \text{on } \partial\Omega^- \cap \partial\Omega_h \end{aligned} \tag{26}$$

$$\begin{aligned} \mathbf{u}^+ - \mathbf{u}^- &= \mathbf{0} \\ \mathbf{B}_h^+ \mathbf{u}^+ + \mathbf{B}_h^- \mathbf{u}^- &= \mathbf{0} \end{aligned} \quad \text{on } \Gamma \tag{27}$$

The solution in each subdomain is approximated by a separate set of basis functions:

$$u_i^h(\mathbf{x}) = \begin{cases} u_i^{h+}(\mathbf{x}) = g_1^+(\mathbf{x}) a_{i1}^+ + \cdots + g_{N_s^+}^+(\mathbf{x}) a_{iN_s^+}^+, & \mathbf{x} \in \bar{\Omega}^+ \\ u_i^{h-}(\mathbf{x}) = g_1^-(\mathbf{x}) a_{i1}^- + \cdots + g_{N_s^-}^-(\mathbf{x}) a_{iN_s^-}^-, & \mathbf{x} \in \bar{\Omega}^- \end{cases} \tag{28}$$

Substituting RBFs approximation in (28) into (25)–(27) and evaluating them at collocation points for *all sub-problems* yields a set of algebraic equations to solve for the coefficients $a_{jI}^{\pm}$.

3.4. Implementation

Let $\tau = \pm$ be the heterogeneity parameter, $\mathbf{P}^\tau$ be a set of N_p^τ collocation points in Ω^τ, $\mathbf{Q}^\tau$ be a set of N_q^τ collocation points on $\partial\Omega^\tau \cap \partial\Omega_g$, $\mathbf{R}^\tau$ be a set of N_r^τ collocation points on $\partial\Omega^\tau \cap \partial\Omega_h$, and $\mathbf{T}$ be a set of N_t collocation points on Γ, we have

$$\begin{aligned} &\mathbf{P}^\tau = \{\mathbf{p}_1^\tau, \mathbf{p}_2^\tau, \ldots, \mathbf{p}_{N_p^\tau}^\tau\} \subseteq \Omega^\tau, \quad \mathbf{Q}^\tau = \{\mathbf{q}_1^\tau, \mathbf{q}_2^\tau, \ldots, \mathbf{q}_{N_q^\tau}^\tau\} \subseteq \partial\Omega^\tau \cap \partial\Omega_g \\ &\mathbf{R}^\tau = \{\mathbf{r}_1^\tau, \mathbf{r}_2^\tau, \ldots, \mathbf{r}_{N_r^\tau}^\tau\} \subseteq \partial\Omega^\tau \cap \partial\Omega_h, \quad \mathbf{T} = \{\mathbf{t}_1, \mathbf{t}_2, \ldots, \mathbf{t}_{N_t}\} \subseteq \Gamma \end{aligned} \tag{29}$$

Let $\mathbf{u}^{h\tau}$ be the approximation function of $\mathbf{u}^\tau$ according to (28) and is expressed as

$$\mathbf{u}^{h\tau} = \boldsymbol{\Phi}^{\tau\mathrm{T}} \mathbf{a}^\tau \tag{30}$$

$$\boldsymbol{\Phi}^{\tau\mathrm{T}} = [\mathbf{g}_1^\tau, \mathbf{g}_2^\tau, \ldots, \mathbf{g}_{N_s^\tau}^\tau], \quad \mathbf{g}_I^\tau = g_I^\tau \mathbf{I}, \quad \mathbf{a}^\tau = [\mathbf{a}_1^\tau, \mathbf{a}_2^\tau, \ldots, \mathbf{a}_{N_s^\tau}^\tau]^{\mathrm{T}}, \quad \mathbf{a}_I^\tau = [\mathbf{a}_{1I}^\tau, \mathbf{a}_{2I}^\tau, \mathbf{a}_{3I}^\tau]^{\mathrm{T}} \tag{31}$$

where g_I^τ is the RBFs with source point $\mathbf{x}_I^\tau \in \bar{\Omega}^\tau$, and $\mathbf{I}$ is an identity matrix. By introducing approximation (30) into strong forms (25)–(27) and evaluating them at the collocation points in the domains, boundaries, and interfaces defined in (29) for the subdomains, we obtain the following discrete equation:

$$\mathbf{A}\mathbf{a} := \begin{bmatrix} \mathbf{A}^+ \\ \mathbf{A}^- \\ \boldsymbol{\Lambda} \end{bmatrix} \mathbf{a} = \begin{bmatrix} \mathbf{b}^+ \\ \mbox{}\mathbf{b}^- \\ \mathbf{0} \end{bmatrix} =: \mathbf{b} \tag{32}$$

DOI: 10.1002/nme

where $\{\mathbf{A}^+, \mathbf{b}^+\}$ and $\{\mathbf{A}^-, \mathbf{b}^-\}$ are the stiffness matrices and force vectors associated with subdomain problems in (25) and (26), respectively, and $\mathbf{\Lambda}$ is associated with the interface conditions in (27). The submatrices and subvectors are defined as

$$\mathbf{A}^+ = \begin{bmatrix} \mathbf{A}_L^+ \\ \mathbf{A}_g^+ \\ \mathbf{A}_h^+ \end{bmatrix}, \quad \mathbf{A}^- = \begin{bmatrix} \mathbf{A}_L^- \\ \mathbf{A}_g^- \\ \mathbf{A}_h^- \end{bmatrix}, \quad \mathbf{\Lambda} = \begin{bmatrix} \mathbf{\Lambda}_g \\ \mathbf{\Lambda}_h \end{bmatrix}, \quad \mathbf{b}^+ = \begin{bmatrix} \mathbf{b}_L^+ \\ \mathbf{b}_g^+ \\ \mathbf{b}_h^+ \end{bmatrix}, \quad \mathbf{b}^- = \begin{bmatrix} \mathbf{b}_L^- \\ \mathbf{b}_g^- \\ \mathbf{b}_h^- \end{bmatrix} \tag{33}$$

where $\mathbf{A}_L^\tau$, $\mathbf{A}_g^\tau$, and $\mathbf{A}_h^\tau$ are the matrices associated with differential operator $\mathbf{L}^\tau$, Dirichlet boundary operator $\mathbf{B}_g^\tau$ and Neumann boundary operator $\mathbf{B}_h^\tau$, respectively, and $\mathbf{\Lambda}_g$ and $\mathbf{\Lambda}_h$ are associated with Dirichlet and Neumann type interface conditions, respectively. The explicit expressions of these matrices and vectors in (32)–(33) are given in the Appendix.

To achieve an optimum convergence, more collocation points than source points need to be used in the discretization. This yields an over-determined system in (32) and is solved by a least-squares method. *It is important to realize that the least-squares solution of strong form collocation in* (32) *is equivalent to the minimization of least-squares functional with quadratures*. We first define the following least-squares method: to seek the approximation solution $\mathbf{u}^h \in U$, where U is the admissible space spanned by the RBFs, such that

$$E(\mathbf{u}^h) = \min_{\mathbf{v}^h \in U} E(\mathbf{v}^h) \tag{34}$$

where

$$\begin{aligned} E(\mathbf{v}^h) = \frac{1}{2} \Bigg\{ & \int_{\Omega^+} (\mathbf{L}^+ \mathbf{v}^{h+} - \mathbf{f}^+)^2 \, \mathrm{d}\Omega + \int_{\Omega^-} (\mathbf{L}^- \mathbf{v}^{h-} - \mathbf{f}^-)^2 \, \mathrm{d}\Omega \\ & + \int_{\partial\Omega_g \cap \partial\Omega^+} (\mathbf{B}_g^+ \mathbf{v}^{h+} - \mathbf{g}^+)^2 \, \mathrm{d}\Gamma + \int_{\partial\Omega_g \cap \partial\Omega^-} (\mathbf{B}_g^- \mathbf{v}^{h-} - \mathbf{g}^-)^2 \, \mathrm{d}\Gamma \\ & + \int_{\partial\Omega_h \cap \partial\Omega^+} (\mathbf{B}_h^+ \mathbf{v}^{h+} - \mathbf{h}^+)^2 \, \mathrm{d}\Gamma + \int_{\partial\Omega_h \cap \partial\Omega^-} (\mathbf{B}_h^- \mathbf{v}^{h-} - \mathbf{h}^-)^2 \, \mathrm{d}\Gamma \\ & + \int_{\Gamma} (\mathbf{v}^{h+} - \mathbf{v}^{h-})^2 \, \mathrm{d}\Gamma + \int_{\Gamma} (\mathbf{B}_h^+ \mathbf{v}^{h+} + \mathbf{B}_h^- \mathbf{v}^{h-})^2 \, \mathrm{d}\Gamma \Bigg\} \end{aligned} \tag{35}$$

where the notation $(\mathbf{y})^2 \equiv (\mathbf{y})^{\mathrm{T}}(\mathbf{y})$. It has been shown in [31] that the errors associated with least-squares method are unbalanced between domain term, Dirichlet boundary term and Neumann boundary term, and a weighted least-squares method has been proposed. In this work, we introduce a weighted version of (35) as

$$\begin{aligned} E(\mathbf{v}^h) = \frac{1}{2} \Bigg\{ & \int_{\Omega^+} (\mathbf{L}^+ \mathbf{v}^{h+} - \mathbf{f}^+)^2 \, \mathrm{d}\Omega + \int_{\Omega^-} (\mathbf{L}^- \mathbf{v}^{h-} - \mathbf{f}^-)^2 \, \mathrm{d}\Omega \\ & + w_g^+ \int_{\partial\Omega_g \cap \partial\Omega^+} (\mathbf{B}_g^+ \mathbf{v}^{h+} - \mathbf{g}^+)^2 \, \mathrm{d}\Gamma + w_g^- \int_{\partial\Omega_g \cap \partial\Omega^-} (\mathbf{B}_g^- \mathbf{v}^{h-} - \mathbf{g}^-)^2 \, \mathrm{d}\Gamma \end{aligned}$$

DOI: 10.1002/nme

$$+w_h^+\int_{\partial\Omega_h\cap\partial\Omega^+}(\mathbf{B}_h^+\mathbf{v}^{h+}-\mathbf{h}^+)^2\,\mathrm{d}\Gamma+w_h^-\int_{\partial\Omega_h\cap\partial\Omega^-}(\mathbf{B}_h^-\mathbf{v}^{h-}-\mathbf{h}^-)^2\,\mathrm{d}\Gamma$$

$$+\bar{w}_g\int_\Gamma(\mathbf{v}^{h+}-\mathbf{v}^{h-})^2\,\mathrm{d}\Gamma+\bar{w}_h\int_\Gamma(\mathbf{B}_h^+\mathbf{v}^{h+}+\mathbf{B}_h^-\mathbf{v}^{h-})^2\,\mathrm{d}\Gamma\Big\} \tag{36}$$

where $w_g^\pm$ and $w_h^\pm$ are the weights associated with Dirichlet and Neumann boundary in each subdomain, respectively, and $\bar{w}_g$ and $\bar{w}_h$ are the weights associated with the two interface conditions on interface Γ. According to [31], the following weights are used:

$$\sqrt{w_g^+}=\sqrt{w_g^-}=\sqrt{\bar{w}_g}=O(\bar{k}\cdot\bar{N}_s),\quad \sqrt{w_h^+}=O(s^+),\quad \sqrt{w_h^-}=O(s^-),\quad \sqrt{\bar{w}_h}=O(1) \tag{37}$$

where $k^\tau=\max(\lambda^\tau,\mu^\tau)$, $\bar{k}=\max(k^+,k^-)$, $\bar{N}_s=\max(N_\mathrm{s}^+,N_\mathrm{s}^-)$, $s^+=\bar{k}/k^+$, $s^-=\bar{k}/k^-$, λ^τ and μ^τ are Lame's constants in $\bar{\Omega}^\tau$, and N_s^τ is the number of source points in $\bar{\Omega}^\tau$. Based on the equivalence of strong form collocation method and the least-squares method with quadratures, the collocation matrices affected by the introduction of weights in (37) are as follows:

$$\mathbf{A}^+=\begin{bmatrix}\mathbf{A}_L^+\\ \sqrt{w_g^+}\mathbf{A}_g^+\\ \sqrt{w_h^+}\mathbf{A}_h^+\end{bmatrix},\quad \mathbf{A}^-=\begin{bmatrix}\mathbf{A}_L^-\\ \sqrt{w_g^-}\mathbf{A}_g^-\\ \sqrt{w_h^-}\mathbf{A}_h^-\end{bmatrix},\quad \mathbf{\Lambda}=\begin{bmatrix}\sqrt{\bar{w}_g}\mathbf{\Lambda}_g\\ \sqrt{\bar{w}_h}\mathbf{\Lambda}_h\end{bmatrix}$$
$$\mathbf{b}^+=\begin{bmatrix}\mathbf{b}_L^+\\ \sqrt{w_g^+}\mathbf{b}_g^+\\ \sqrt{w_h^+}\mathbf{b}_h^+\end{bmatrix},\quad \mathbf{b}^-=\begin{bmatrix}\mathbf{b}_L^-\\ \sqrt{w_g^-}\mathbf{b}_g^-\\ \sqrt{w_h^-}\mathbf{b}_h^-\end{bmatrix} \tag{38}$$

The above-weighted functional problem in (36) can be described equivalently

$$a(\mathbf{v}^h,\mathbf{u}^h)=f(\mathbf{v}^h)\quad\forall\mathbf{v}^h\in U \tag{39}$$

where the bilinear and linear forms are defined as follows:

$$a(\mathbf{v}^h,\mathbf{u}^h)=\int_{\Omega^\pm}(\mathbf{L}^\pm\mathbf{v}^{h\pm})^\mathrm{T}(\mathbf{L}^\pm\mathbf{u}^{h\pm})\,\mathrm{d}\Omega+w_g^\pm\int_{\partial\Omega_g\cap\partial\Omega^\pm}(\mathbf{B}_g^\pm\mathbf{v}^{h\pm})^\mathrm{T}(\mathbf{B}_g^\pm\mathbf{u}^{h\pm})\,\mathrm{d}\Gamma$$

$$+w_h^\pm\int_{\partial\Omega_h\cap\partial\Omega^\pm}(\mathbf{B}_h^\pm\mathbf{v}^{h\pm})^\mathrm{T}(\mathbf{B}_h^\pm\mathbf{u}^{h\pm})\,\mathrm{d}\Gamma+\bar{w}_g\int_\Gamma(\mathbf{v}^{h+}-\mathbf{v}^{h-})^\mathrm{T}(\mathbf{u}^{h+}-\mathbf{u}^{h-})\,\mathrm{d}\Gamma$$

$$+\bar{w}_h\int_\Gamma(\mathbf{B}_h^+\mathbf{v}^{h+}+\mathbf{B}_h^-\mathbf{v}^{h-})^\mathrm{T}(\mathbf{B}_h^+\mathbf{u}^{h+}+\mathbf{B}_h^-\mathbf{u}^{h-})\,\mathrm{d}\Gamma \tag{40}$$

and

$$f(\mathbf{v}^h)=\int_{\Omega^\pm}(\mathbf{L}^\pm\mathbf{v}^{h\pm})^\mathrm{T}\mathbf{f}^\pm\,\mathrm{d}\Omega+w_g^\pm\int_{\partial\Omega_g\cap\partial\Omega^\pm}(\mathbf{B}_g^\pm\mathbf{v}^{h\pm})^\mathrm{T}\mathbf{g}^\pm\,\mathrm{d}\Gamma$$

$$+w_h^\pm\int_{\partial\Omega_h\cap\partial\Omega^\pm}(\mathbf{B}_h^\pm\mathbf{v}^{h\pm})^\mathrm{T}\mathbf{h}^\pm\,\mathrm{d}\Gamma \tag{41}$$

DOI: 10.1002/nme

Here, we used $\int_{\Omega^\pm}(\mathbf{L}^\pm\mathbf{v}^{h\pm})^{\mathrm{T}}(\mathbf{L}^\pm\mathbf{u}^{h\pm})\,\mathrm{d}\Omega$ to denote $\int_{\Omega^+}(\mathbf{L}^+\mathbf{v}^{h+})^2\,\mathrm{d}\Omega+\int_{\Omega^-}(\mathbf{L}^-\mathbf{v}^{h-})^2\,\mathrm{d}\Omega$, and same notation applies to other terms. The integrals given in the above least-squares problem can be approximated by Newton–Cotes integration rules, that is to seek $\tilde{\mathbf{u}}^h\in U$ such that

$$\tilde{a}(\mathbf{v}^h,\tilde{\mathbf{u}}^h)=\tilde{f}(\mathbf{v}^h)\quad\forall\mathbf{v}^h\in U \tag{42}$$

It is equivalent to seek $\tilde{\mathbf{u}}^h\in U$ that satisfies

$$\tilde{E}(\tilde{\mathbf{u}}^h)=\min_{\mathbf{v}^h\in U}\tilde{E}(\mathbf{v}^h) \tag{43}$$

Here, we denote $\tilde{E}=\int^\wedge(\cdot)$ the numerical integration counterpart of $E=\int(\cdot)$, where $\int^\wedge(\cdot)$ denotes numerical integration. Same notation applies to $\tilde{a}(\cdot,\cdot)$ and $\tilde{f}(\cdot)$. Recall that the least-squares solution of strong form collocation is equivalent to the minimization of least-squares functional with quadratures. Thus, the minimization of subdomain weighted least-squares functional in (43) and (36) leads to a subdomain weighted collocation method in (32). Further, the convergence properties of strong form collocation method can be obtained by analyzing least-squares functional as follows.

To start, define the following norm:

$$\begin{aligned}\|\mathbf{v}^h\|_E^2=\bar{k}\|\mathbf{v}^{h\pm}\|_{1,\Omega^\pm}^2+\|\mathbf{L}^\pm\mathbf{v}^{h\pm}\|_{0,\Omega^\pm}^2+w_g^\pm\|\mathbf{B}_g^\pm\mathbf{v}^{h\pm}\|_{0,\partial\Omega_g\cap\partial\Omega^\pm}^2+w_h^\pm\|\mathbf{B}_h^\pm\mathbf{v}^{h\pm}\|_{0,\partial\Omega_h\cap\partial\Omega^\pm}^2\\ +\bar{w}_g\|\mathbf{v}^{h+}-\mathbf{v}^{h-}\|_{0,\Gamma}^2+\bar{w}_h\|\mathbf{B}_h^+\mathbf{v}^{h+}+\mathbf{B}_h^-\mathbf{v}^{h-}\|_{0,\Gamma}^2\end{aligned} \tag{44}$$

where $w_g^\pm\|\mathbf{B}_g^\pm\mathbf{v}^{h\pm}\|_{0,\partial\Omega_g\cap\partial\Omega^\pm}^2=w_g^+\|\mathbf{B}_g^+\mathbf{v}^{h+}\|_{0,\partial\Omega_g\cap\partial\Omega^+}^2+w_g^-\|\mathbf{B}_g^-\mathbf{v}^{h-}\|_{0,\partial\Omega_g\cap\partial\Omega^-}^2$, etc, $\bar{k}=\max(\lambda^\pm,\mu^\pm)$. To show that there exists an optimal solution we need the following theorem.

Theorem 3.1
Suppose that the bilinear form $\tilde{a}(\cdot,\cdot)$ is continuous and coercive in U

$$\tilde{a}(\mathbf{v}^h,\mathbf{u}^h)\leqslant C_1\|\mathbf{v}^h\|_E\|\mathbf{u}^h\|_E\quad\forall\mathbf{v}^h\in U \tag{45}$$

$$\tilde{a}(\mathbf{u}^h,\mathbf{u}^h)\geqslant C_2\|\mathbf{u}^h\|_E^2\quad\forall u^h\in U \tag{46}$$

where C_1 and C_2 are positive constants independent of the number of collocation points.

By using the Lax-Milgram lemma, it can be shown that the solution of the subdomain weighted collocation method has error bound:

$$\|\mathbf{u}-\tilde{\mathbf{u}}^h\|_E\leqslant C\inf_{\mathbf{v}^h\in U}\|\mathbf{u}-\mathbf{v}^h\|_E \tag{47}$$

Detail analysis is given in the next section.

DOI: 10.1002/nme

4. ERROR ANALYSIS OF SUBDOMAIN RBCM FOR HETEROGENEOUS MEDIA

We rewrite that the weighted least-squares functional (36) corresponds to the subdomain collocation Equations (32)–(33) as follows:

$$E(\mathbf{u}^h)=\sum_{i=1}^{n} E(\mathbf{u}^{h(i)}),\quad \mathbf{u}^h\in U=V\times V\times V \tag{48}$$

where n is the number of subdomains, $V=V^{(1)}\times\cdots\times V^{(n)}$, and $V^{(i)}=\text{span}\{g_1^{(i)},g_2^{(i)},\ldots,g_{N_s^{(i)}}^{(i)}\}$. For simplicity, we consider the total domain consisting only two subdomains denoted as $\bar{\Omega}^+=\Omega^+\cup\partial\Omega^+$ and $\bar{\Omega}^-=\Omega^-\cup\partial\Omega^-$, $\bar{\Omega}^+\cup\bar{\Omega}^-=\bar{\Omega}$, and $\partial\bar{\Omega}^+\cap\partial\bar{\Omega}^-=\Gamma$ is the interface with surface outward normals $\mathbf{n}^+$ and $\mathbf{n}^-$ defined in Figure 2.

The weighted least-squares functional is expressed as

$$\begin{aligned}E(\mathbf{u}^h)=\frac{1}{2}\Bigg\{&\int_{\Omega^\pm}(\sigma_{ij,j}^\pm+b_i^\pm)^2\,\mathrm{d}\Omega+w_h^\pm\int_{\partial\Omega_h\cap\partial\Omega^\pm}(\sigma_{ij}^\pm n_j^\pm-h_i^\pm)^2\,\mathrm{d}\Gamma+w_g^\pm\int_{\partial\Omega_g\cap\partial\Omega^\pm}(u_i^{h\pm}-g_i^\pm)^2\,\mathrm{d}\Gamma\\&+\bar{w}_h\int_\Gamma(\sigma_{ij}^+n_j-\sigma_{ij}^-n_j)^2\,\mathrm{d}\Gamma+\bar{w}_g\int_\Gamma(u_i^{h+}-u_i^{h-})^2\,\mathrm{d}\Gamma\Bigg\}\end{aligned} \tag{49}$$

Here, we use the notation $(y_i)^2\equiv y_iy_i$, $\sigma_{ij}^\pm=C_{ijk\ell}^\pm u_{(k,\ell)}^{h\pm}$ is the stress tensor, $n_i=n_i^+=-n_i^-$, $w_g^\pm$ and $w_g^\pm$ are the boundary weights, and $\bar{w}_g$ and $\bar{w}_h$ are the interface weights as described in Section 3. We also denote $\int_{\Omega^\pm}(\sigma_{ij,j}^\pm+b_i^\pm)^2\,\mathrm{d}\Omega=\int_{\Omega^+}(\sigma_{ij,j}^++b_i^+)^2\,\mathrm{d}\Omega+\int_{\Omega^-}(\sigma_{ij,j}^-+b_i^-)^2\,\mathrm{d}\Omega$, etc. to simplify the expression of the equation. We seek $\mathbf{u}^h$ that minimizes the functional:

$$E(\mathbf{u}^h)=\min_{\mathbf{v}^h\in U}E(\mathbf{v}^h) \tag{50}$$

This minimization problem is equivalent to

$$a(\mathbf{v}^h,\mathbf{u}^h)=f(\mathbf{v}^h)\quad\forall\mathbf{v}^h\in U \tag{51}$$

where the bilinear form is

$$\begin{aligned}a(\mathbf{v}^h,\mathbf{u}^h)=&\int_{\Omega^\pm}\eta_{ik,k}^\pm\sigma_{ij,j}^\pm\,\mathrm{d}\Omega+w_g^\pm\int_{\partial\Omega_g\cap\partial\Omega^\pm}v_i^{h\pm}u_i^{h\pm}\,\mathrm{d}\Gamma\\&+w_h^\pm\int_{\partial\Omega_h\cap\partial\Omega^\pm}\eta_{ik}^\pm n_k^\pm\sigma_{ij}^\pm n_j^\pm\,\mathrm{d}\Gamma+\bar{w}_g\int_\Gamma(v_i^{h+}-v_i^{h-})(u_i^{h+}-u_i^{h-})\,\mathrm{d}\Gamma\\&+\bar{w}_h\int_\Gamma(\eta_{ik}^+n_k-\eta_{ik}^-n_k)(\sigma_{ij}^+n_j-\sigma_{ij}^-n_j)\,\mathrm{d}\Gamma\end{aligned} \tag{52}$$

$\eta_{ij}^\pm=C_{ijk\ell}^\pm v_{(k,\ell)}^{h\pm}$, and the linear form

$$f(\mathbf{v}^h)=-\int_{\Omega^\pm}\eta_{ij,j}^\pm b_i^\pm\,\mathrm{d}\Omega+w_g^\pm\int_{\partial\Omega_g\cap\partial\Omega^\pm}v_i^{h\pm}g_i^\pm\,\mathrm{d}\Gamma+w_h^\pm\int_{\partial\Omega_h\cap\partial\Omega^\pm}\eta_{ij}^\pm n_j^\pm h_i^\pm\,\mathrm{d}\Gamma \tag{53}$$

DOI: 10.1002/nme

We define the following norm as the elasticity counterpart of the norm defined in (44):

$$\|\mathbf{u}^h\|_H = \sum_{i=1}^{3}\{\bar{\alpha}\|u_i^h\|_{1,\Omega}^2+\|\sigma_{ij,j}^{\pm}\|_{0,\Omega^{\pm}}^2+\bar{w}_g\|u_i^{h+}-u_i^{h-}\|_{0,\Gamma}^2$$
$$+\bar{w}_h\|\sigma_{ij}^{+}n_j-\sigma_{ij}^{-}n_j\|_{0,\Gamma}^2+w_h^{\pm}\|\sigma_{ij}^{\pm}n_j^{\pm}\|_{0,\partial\Omega_h\cap\partial\Omega^{\pm}}^2+w_g^{\pm}\|u_i^{h\pm}\|_{0,\partial\Omega_g\cap\partial\Omega^{\pm}}^2\}^{1/2} \quad (54)$$

where $\bar{\alpha}=\min(\alpha^+,\alpha^-)$, $\alpha^{\pm}=\min(\lambda^{\pm},\mu^{\pm})$ and

$$\bar{\alpha}\|u_i^h\|_{1,\Omega}^2=\bar{\alpha}\|u_i^{h+}\|_{1,\Omega^+}^2+\bar{\alpha}\|u_i^{h-}\|_{1,\Omega^-}^2 \quad (55)$$

There exist a few useful lemmas summarized below.

Lemma 4.1
Let $u_i^{h\pm}$ be the components of the solution $\mathbf{u}^{h\pm}$ in subdomains $\Omega^{\pm}$, respectively, there exist the following trace inequalities:

$$\begin{aligned}\|u_i^{h\pm}\|_{0,\Gamma} &\leqslant C\|u_i^h\|_{1,\Omega}\\ \|\sigma_{ij}^{\pm}n_j\|_{0,\Gamma} &\leqslant CN_s^{\pm}\sqrt{\bar{k}}\|u_i^h\|_{1,\Omega}\\ \|u_i^{h\pm}\|_{0,\partial\Omega g\cap\partial\Omega^{\pm}} &\leqslant C\|u_i^h\|_{1,\Omega}\\ \|\sigma_{ij}^{\pm}n_j^{\pm}\|_{0,\partial\Omega_h\cap\partial\Omega^{\pm}} &\leqslant C\bar{N}_s\sqrt{\bar{k}}\|u_i^h\|_{1,\Omega}\end{aligned} \quad (56)$$

where $\bar{k}=\max\{k^+,k^-\}$, $\bar{N}_s=\max\{N_s^+,N_s^-\}$, and C is a generic constant independent of N_s^+, N_s^-, $\bar{N}_s$, and $\bar{k}$. The above trace inequalities can be found in References [32, 33].

Remark 4.1
Since $\Omega=\Omega^+\cup\Omega^-\cup\Gamma$, using integration by parts we have

$$\begin{aligned}\bar{\alpha}|u_i^h|_{1,\Omega}^2 &\leqslant \int_{\Omega}u_{i,j}^h\sigma_{ij}\,\mathrm{d}\Omega=-\int_{\Omega}u_i^h\sigma_{ij,j}\,\mathrm{d}\Omega+\int_{\partial\Omega}u_i^h\sigma_{ij}n_j\,\mathrm{d}\Gamma\\ &=-\int_{\Omega^+}u_i^{h+}\sigma_{ij,j}^{+}\,\mathrm{d}\Omega-\int_{\Omega^-}u_i^{h-}\sigma_{ij,j}^{-}\,\mathrm{d}\Omega+\int_{\partial\Omega^+}u_i^{h+}\sigma_{ij}^{+}n_j^{+}\,\mathrm{d}\Gamma\\ &\quad+\int_{\partial\Omega^-}u_i^{h-}\sigma_{ij}^{-}n_j^{-}\,\mathrm{d}\Gamma\end{aligned} \quad (57)$$

Since $\partial\Omega=\partial\Omega^+\cup\partial\Omega^-=\partial\Omega_g\cup\partial\Omega_h\cup\Gamma$, and considering $n_j=n_j^+=-n_j^-$ on the interface Γ, the third and fourth terms on the right-hand side of above equation can be rearranged as

$$\begin{aligned}&\int_{\partial\Omega^+}u_i^{h+}\sigma_{ij}^{+}n_j^{+}\,\mathrm{d}\Gamma+\int_{\partial\Omega^-}u_i^{h-}\sigma_{ij}^{-}n_j^{-}\,\mathrm{d}\Gamma\\ &=\int_{\partial\Omega_h\cap\partial\Omega^{\pm}}u_i^{h\pm}\sigma_{ij}^{\pm}n_j^{\pm}\,\mathrm{d}\Gamma+\int_{\partial\Omega_g\cap\partial\Omega^{\pm}}u_i^{h\pm}\sigma_{ij}^{\pm}n_j^{\pm}\,\mathrm{d}\Gamma+\int_{\Gamma}u_i^{h+}\sigma_{ij}^{+}n_j^{+}\,\mathrm{d}\Gamma+\int_{\Gamma}u_i^{h-}\sigma_{ij}^{-}n_j^{-}\,\mathrm{d}\Gamma\\ &=\int_{\partial\Omega_h\cap\partial\Omega^{\pm}}u_i^{h\pm}\sigma_{ij}^{\pm}n_j^{\pm}\,\mathrm{d}\Gamma+\int_{\partial\Omega_g\cap\partial\Omega^{\pm}}u_i^{h\pm}\sigma_{ij}^{\pm}n_j^{\pm}\,\mathrm{d}\Gamma+\int_{\Gamma}(u_i^{h+}\sigma_{ij}^{+}n_j-u_i^{h-}\sigma_{ij}^{-}n_j)\,\mathrm{d}\Gamma\end{aligned}$$

DOI: 10.1002/nme

$$= \int_{\partial\Omega_h \cap \partial\Omega^{\pm}} u_i^{h\pm} \sigma_{ij}^{\pm} n_j^{\pm} \, \mathrm{d}\Gamma + \int_{\partial\Omega_g \cap \partial\Omega^{\pm}} u_i^{h\pm} \sigma_{ij}^{\pm} n_j^{\pm} \, \mathrm{d}\Gamma$$

$$+ \int_{\Gamma} (u_i^{h+} - u_i^{h-}) \sigma_{ij}^{+} n_j \, \mathrm{d}\Gamma + \int_{\Gamma} (\sigma_{ij}^{+} n_j - \sigma_{ij}^{-} n_j) u_i^{h-} \, \mathrm{d}\Gamma \tag{58}$$

It follows that

$$\bar{\alpha} |u_i^h|_{1,\Omega}^2 \leqslant \|u_i^{h\pm}\|_{0,\Omega^{\pm}} \|\sigma_{ij,j}^{\pm}\|_{0,\Omega^{\pm}} + \|u_i^{h+} - u_i^{h-}\|_{0,\Gamma} \|\sigma_{ij}^{+} n_j\|_{0,\Gamma} + \|\sigma_{ij}^{+} n_j - \sigma_{ij}^{-} n_j\|_{0,\Gamma} \|u_i^{h-}\|_{0,\Gamma}$$

$$+ \|u_i^{h\pm}\|_{0,\partial\Omega_h \cap \partial\Omega^{\pm}} \|\sigma_{ij}^{\pm} n_j^{\pm}\|_{0,\partial\Omega_h \cap \partial\Omega^{\pm}} + \|u_i^{h\pm}\|_{0,\partial\Omega_g \cap \partial\Omega^{\pm}} \|\sigma_{ij}^{\pm} n_j^{\pm}\|_{0,\partial\Omega_g \cap \partial\Omega^{\pm}} \tag{59}$$

It can be seen that both the displacement and the traction continuity conditions on the interface exist in (59). They are critical in proving the coercivity in Lemma 4.2. The above analysis also explains the reasons how interface conditions are added to the least-squares functional, the bilinear form, and energy norm in Section 3.

By using the results stated in Lemma 4.1 and in (59) and the Poincare inequality, we have the following lemma.

Lemma 4.2
There exists a positive number $\bar{\alpha}$ such that the bilinear form $a(\cdot, \cdot)$ satisfies the following condition:

$$\bar{\alpha} \|\mathbf{u}^h\|_{1,\Omega}^2 \leqslant C_0 a(\mathbf{u}^h, \mathbf{u}^h) \quad \forall \mathbf{u}^h \in U \tag{60}$$

where C_0 is a generic constant independent of N_s^+, N_s^-, $\bar{N}_s$, and $\bar{k}$.

We have used the relationship between 1-norm and bilinear form to yield (60), see [33]. To obtain an optimal solution of the subdomain weighted collocation method, the results given in Lemma 4.2 and the Lax-Milgram lemma will be used.

Lemma 4.3
Suppose that the bilinear form $a(\cdot, \cdot)$ is continuous and coercive in U, we have

$$\begin{aligned} a(\mathbf{v}^h, \mathbf{u}^h) &\leqslant C_1 \|\mathbf{v}^h\|_H \|\mathbf{u}^h\|_H \quad \forall \mathbf{v}^h \in U \\ a(\mathbf{u}^h, \mathbf{u}^h) &\geqslant C_2 \|\mathbf{u}^h\|_H^2 \quad \forall \mathbf{u}^h \in U \end{aligned} \tag{61}$$

where C_1 and C_2 are two positive constants independent of N_s^+, N_s^-, $\bar{N}_s$, and $\bar{k}$. As such, there is an optimal solution $\mathbf{u}^h$ for the subdomain weighted least-squares method:

$$\|\mathbf{u} - \mathbf{u}^h\|_H \leqslant C \inf_{\mathbf{v}^h \in U} \|\mathbf{u} - \mathbf{v}^h\|_H \tag{62}$$

Since the Newton–Cotes integration rules are used in the functional, we summarize the error bounds for the approximation in following lemmas.

Remark 4.2
To arrive (61), the Poincare inequality [34], trace inequalities in (56) [32] and the result in (59) [33] have been used. These inequalities yield the relationship between H-norm and bilinear form, that is, the coercivity. Although [33] deals with Poisson problem, the proof can be easily extended to elasticity.

DOI: 10.1002/nme

Lemma 4.4
Let r be the order of polynomial that the numerical integration can exactly integrate. There exist the following bounds for the approximate integrals:

$$\begin{aligned}
\left|\left(\int_{\Omega^\pm}^{\wedge}-\int_{\Omega^\pm}\right)(\sigma_{ij,j}^{\pm})^2\right| &\leqslant Ck\hbar^{r+1}(N_s^{\pm})^{r+5}\|u_i^{h\pm}\|_{0,\Omega^\pm}^2\\
\left|\left(\int_{\partial\Omega_g\cap\partial\Omega^\pm}^{\wedge}-\int_{\partial\Omega_g\cap\partial\Omega^\pm}\right)(u_i^{\pm})^2\right| &\leqslant C\hbar^{r+1}\bar{N}_s^{r+1}\|u_i^{h\pm}\|_{0,\partial\Omega_g\cap\partial\Omega^\pm}^2\\
\left|\left(\int_{\partial\Omega_h\cap\partial\Omega^\pm}^{\wedge}-\int_{\partial\Omega_h\cap\partial\Omega^\pm}\right)(\sigma_{ij}^{\pm}n_j^{\pm})^2\right| &\leqslant Ck\hbar^{r+1}\bar{N}_s^{r+3}\|u_i^{h\pm}\|_{0,\partial\Omega_h\cap\partial\Omega^\pm}^2\\
\left|\left(\int_{\Gamma}^{\wedge}-\int_{\Gamma}\right)(u_i^{h+}-u_i^{h-})^2\right| &\leqslant C_1\hbar^{r+1}(N_s^{+})^{r+1}\|u_i^{h+}\|_{0,\Gamma}^2+C_2\hbar^{r+1}(N_s^{-})^{r+1}\|u_i^{h-}\|_{0,\Gamma}^2\\
\left|\left(\int_{\Gamma}^{\wedge}-\int_{\Gamma}\right)(\sigma_{ij}^{+}n_j-\sigma_{ij}^{-}n_j)^2\right| &\leqslant C_1k\hbar^{r+1}(N_s^{+})^{r+3}\|u_i^{h+}\|_{0,\Gamma}^2\\
&\quad +C_2k\hbar^{r+1}(N_s^{-})^{r+3}\|u_i^{h-}\|_{0,\Gamma}^2
\end{aligned}\tag{63}$$

where $\int_{\Omega^+}^{\wedge}$ denotes the approximation of $\int_{\Omega^+}$, $\bar{N}_s=\max\{N_s^+, N_s^-\}$, $\hbar=\max\{\hbar_i\}$, where $\hbar_i$ is the maximal distance of integration nodes (collocation points) and its neighbors.

Lemma 4.5
Suppose the conditions in Lemmas 4.3 and 4.4 hold, we choose $\hbar$ to satisfy

$$\hbar^{r+1}\bar{N}_s^{r+3}=O(1)\tag{64}$$

Then, there exist the following inequalities:

$$\begin{aligned}
&\tilde{a}(\mathbf{v}^h,\mathbf{u}^h)\leqslant\tilde{C}_1\|\mathbf{v}^h\|_H\|\mathbf{u}^h\|_H \quad \forall\mathbf{v}^h\in U\\
&\tilde{a}(\mathbf{u}^h,\mathbf{u}^h)\geqslant\tilde{C}_2\|\mathbf{u}^h\|_H^2 \quad \forall\mathbf{u}^h\in U
\end{aligned}\tag{65}$$

where $\tilde{a}(\cdot,\cdot)$ is the integration counterpart of $a(\cdot,\cdot)$, and $\tilde{C}_1, \tilde{C}_2$ are generic constants independent of $N_s^+, N_s^-, \bar{N}_s$, and $\bar{k}$.

Under the conditions given in (64), and consider that $\hbar=\bar{N}_s^{-1}$, we have $\hbar=O(h^{[1+2/(1+r)]})$. This indicates that for a desired accuracy, the density of collocation points should be selected much denser than the source points i.e. $N_c\geqslant N_s$ especially when lower-order quadrature rules are used. Finally, we have the following important theorem.

Theorem 4.1
Suppose that the bilinear form $\tilde{a}(\cdot,\cdot)$ is continuous and coercive in U, then the solution of the subdomain weighted collocation method has error bound

$$\|\mathbf{u}-\tilde{\mathbf{u}}^h\|_H\leqslant C\inf_{\mathbf{v}^h\in U}\|\mathbf{u}-\mathbf{v}^h\|_H\tag{66}$$

DOI: 10.1002/nme

Moreover,

$$\|\mathbf{u}-\tilde{\mathbf{u}}^h\|_H \leqslant C\sum_{i=1}^{3}\{\sqrt{\bar{\alpha}}\|u_i^{\pm}-v_i^{h\pm}\|_{1,\Omega^{\pm}}+\|\sigma_{ij,j}^{\pm}-\eta_{ij.j}^{\pm}\|_{0,\Omega^{\pm}}+\sqrt{\bar{w}_g}\|v_i^{h+}-v_i^{h-}\|_{0,\Gamma}$$

$$+\sqrt{\bar{w}_h}\|(\eta_{ij}^{+}-\eta_{ij}^{-})n_j\|_{0,\Gamma}+\sqrt{w_g^{\pm}}\|u_i^{\pm}-v_i^{h\pm}\|_{0,\partial\Omega_g\cap\partial\Omega^{\pm}}$$

$$+\sqrt{w_h^{\pm}}\|(\sigma_{ij}^{\pm}-\eta_{ij}^{\pm})n_j\|_{0,\partial\Omega_h\cap\partial\Omega^{\pm}}\} \tag{67}$$

where $\eta_{ij}^{\pm}$ is the stress calculated by $v_i^{h\pm}$, and C is a generic constant.

Remark 4.3
Both displacement and traction continuity conditions on the interface are needed to prove the coercivity in Lemmas 4.2, 4.3, 4.5 and in Theorem 4.1, and to yield an optimal solution $\tilde{\mathbf{u}}^h$. If RBCM exhibits exponential convergence in homogeneous problem, same convergence properties exist in subdomain radial basis collocation method (SD-RBCM) if the errors on the material interfaces are well controlled.

5. NUMERICAL EXAMPLES

In the following study, we consider two types of approximation functions:

(a) Reciprocal multiquadrics RBFs:

$$g_I(\mathbf{x})=(r_I^2+c^2)^{-1/2},\quad r_I=\sqrt{(x-x_I)^2+(y-y_I)^2} \tag{68}$$

(b) L-RBFs constructed based on partition of unity with RK as the localizing function given in Equation (4), where the RK is constructed using cubic bases and a quintic spline (C^4 continuity) kernel function:

$$\varphi(s)=\begin{cases}\dfrac{11}{20}-\dfrac{s^2}{2}+\dfrac{s^4}{4}-\dfrac{s^5}{12}, & 0\leqslant s<1,\\[2ex] \dfrac{17}{40}+\dfrac{5s}{8}-\dfrac{7s^2}{4}+\dfrac{5s^3}{4}-\dfrac{3s^4}{8}+\dfrac{s^5}{24}, & 1\leqslant s<2,\\[2ex] \dfrac{243}{120}-\dfrac{81s}{24}+\dfrac{9s^2}{4}-\dfrac{3s^3}{4}+\dfrac{s^4}{8}-\dfrac{s^5}{120}, & 2\leqslant s<3,\\[2ex] 0, & s\geqslant 3,\end{cases}\qquad s=\frac{\|\mathbf{x}-\mathbf{x}_I\|}{a} \tag{69}$$

In the following examples, c denotes the shape parameters in RBFs, h represents the nodal distance, and a is the radius of finite cover in the L-RBFs. We use the following methods in the numerical examples:

1. Radial basis collocation method (RBCM): nonlocal multiquadrics RBFs as approximation in conjunction with collocation of strong form.

DOI: 10.1002/nme

2. Subdomain radial basis collocation method (SD-RBCM): nonlocal multiquadrics RBFs as approximation in conjunction with subdomain collocation of strong form.
3. Subdomain localized radial basis collocation method (SD-LRBCM): L-RBFs as approximation in conjunction with subdomain collocation of strong form.

In all examples, the density of collocation points about twice the density of the source points in each dimension is used [33, 35], unless specified otherwise. In the discussion of numerical results, errors are measured by L2-norm and H1-norm defined as

$$\|\mathbf{u}^h-\mathbf{u}\|_0=\left(\int_\Omega (u_i^h-u_i)(u_i^h-u_i)\,\mathrm{d}\Omega\right)^{1/2} \tag{70}$$

$$|\mathbf{u}^h-\mathbf{u}|_1=\left(\int_\Omega (u_{i,j}^h-u_{i,j})(u_{i,j}^h-u_{i,j})\,\mathrm{d}\Omega\right)^{1/2} \tag{71}$$

5.1. One-dimensional bi-material rod

We repeat the one-dimensional bi-material rod as discussed in (6)–(7) in Section 3.1, and consider existence of body force conditions: (1) $b(x)=0$, (2) $b(x)=1.5^x$.

As discussed in Sections 3 and 4, both displacement continuity and traction equilibrium conditions should be imposed on the material interface Γ. We denote $\Omega^+:=\{x:0<x<5\}$, $\Omega^-:=\{x:5<x<10\}$, and material interface $\Gamma:=\{x:x=5\}$. To numerically verify this condition, we consider the following three interface conditions:

Interface condition I:

$$\sigma^+=\sigma^- \quad \text{on } \Gamma \tag{72}$$

Interface condition II:

$$u^+=u^- \quad \text{on } \Gamma \tag{73}$$

Interface condition III:

$$\begin{aligned}\sigma^+&=\sigma^- \quad \text{on } \Gamma\\ u^+&=u^- \quad \text{on } \Gamma\end{aligned} \tag{74}$$

Note that traction continuity $\sigma_{ij}^+n_j^++\sigma_{ij}^-n_j^-=0$ has been simplified to $\sigma^+=\sigma^-$ in one dimension. In this numerical test, uniform source point distribution is used, and $N_s=41$. Guiding by Equation (37), we use weights $\sqrt{w_g^+}=\sqrt{w_g^-}=\sqrt{\bar{w}_g}=10^5$, $\sqrt{w_h^+}=10$, $\sqrt{w_h^-}=1$, $\sqrt{\bar{w}_h}=1$ in the weighted collocation. The comparison of solutions for the case of zero body force obtained by SD-RBCM using different interface conditions is shown in Figure 3. The results clearly indicate that the imposition of both displacement continuity and traction equilibrium conditions yields the best accuracy. Imposition of only one of the two conditions results in errors. We will use both displacement and traction interface conditions for the remaining numerical examples when subdomain collocation method is used.

The results obtained from domain RBCM and SD-RBCM are shown in Figure 4. As expected, RBCM does not capture material interface, whereas SD-RBCM is substantially accurate.

DOI: 10.1002/nme

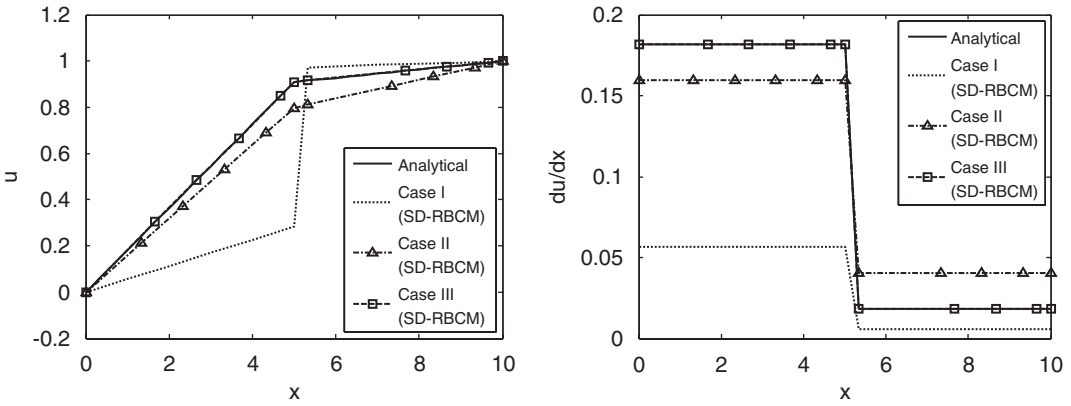

Figure 3. Bi-material elastic rod subjected to zero body force analyzed by SD-RBCM using different interface conditions.

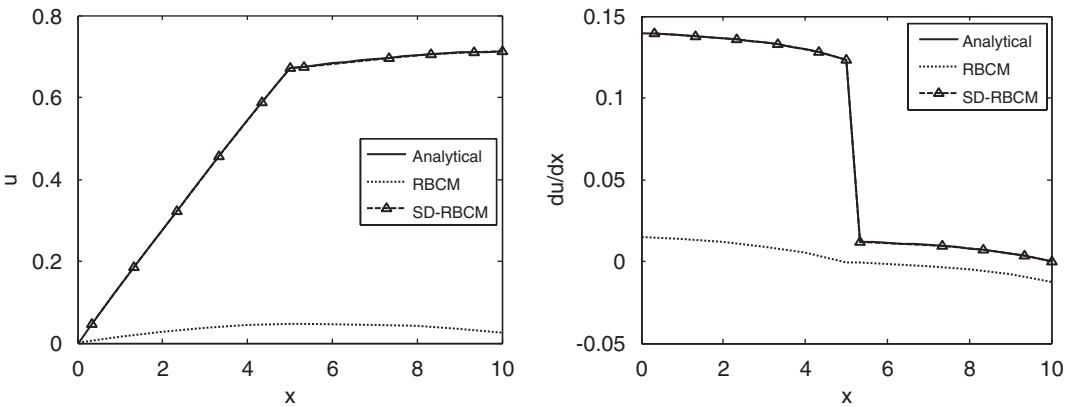

Figure 4. Bi-material elastic rod subjected to higher-order body force obtained by RBCM and SD-RBCM.

The comparison of L2- and H1-norms of RBCM and SD-RBCM are shown in Figure 5. This problem reveals that the use of subdomain collocation is critical in capturing the local material interface behavior when nonlocal RBFs are used.

5.2. Two-dimensional bi-material plate

A rectangular plate composed of two materials is subjected to a uniform tension $h=1.0$ in the horizontal direction as shown in Figure 6. All points on the left edge of the plate are fixed in the horizontal direction and free to move in the vertical direction, and all points on the bottom edge are free to move in the horizontal direction and fixed in the vertical direction. The material properties are: Young's moduli $E^+=1\times10^3$, $E^-=1\times10^4$, and the Poisson ratios $v^+=0.25$, $v^-=0.3$. This problem is different from problem 5.1 due to the Poisson effect that yields a local 'boundary layer' effect as will be seen below.

DOI: 10.1002/nme

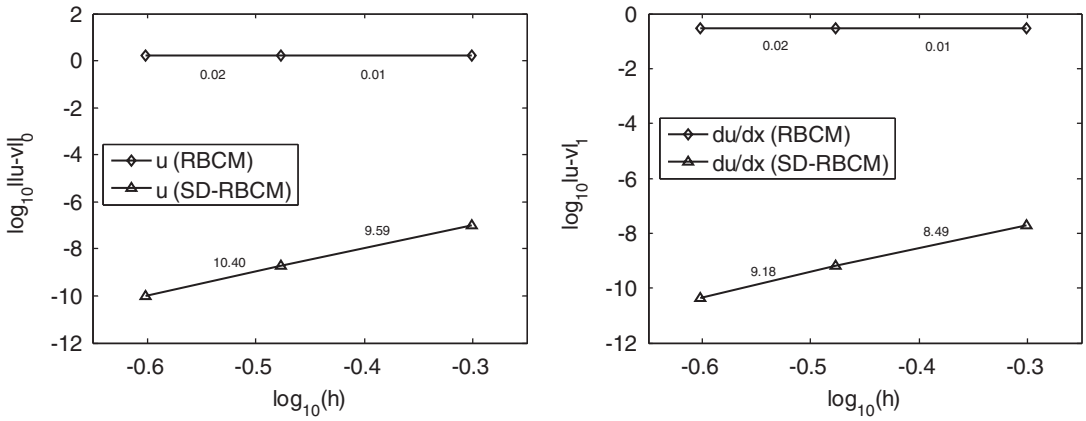

Figure 5. Convergence of L2- and H1-error norms of bi-material elastic rod with body force using RBCM and SD-RBCM.

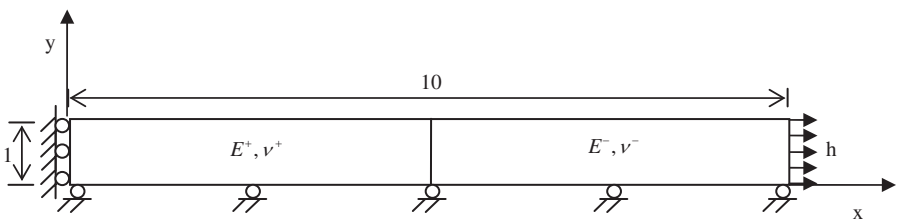

Figure 6. Bi-material plate subjected to tension.

The domain is discretized by 90×9 uniform source points (N_s), and 180×18 uniform collocation points (N_c). The weights for the weighted collocation are $\sqrt{w_g^+} = \sqrt{w_g^-} = \sqrt{\bar{w}_g} = 10^5$, $\sqrt{w_h^+} = 10$, $\sqrt{w_h^-} = 1$, $\sqrt{\bar{w}_h} = 1$. Finite element solution with 16 000 nodes is used as the reference solution. The solutions along $y = 0.5$ of FEM (16 000 nodes), RBCM, SD-RBCM, and SD-LRBCM are compared in Figure 7. The results show again that RBCM solution is very poor. Owing to the very localized thin layer of stress concentration near the material interface, SD-RBCM also yields considerable errors in the stress solutions. The localized stresses can be better captured by the use of L-RBFs in SD-LRBCM. The comparison of L2- and H1-error norms generated by RBCM, SD-RBCM, and SD-LRBCM is shown in Figure 8, where RBCM and SD-RBCM do not converge for this problem, and SD-LRBCM generates the best convergence among the three methods.

5.3. Plate with circular inclusion

A plate with a circular inclusion subjected to far-field horizontal traction $\sigma_0 = 1.0$ is shown in Figure 9. The interface between the two materials is assumed to be perfectly bonded. The material

DOI: 10.1002/nme

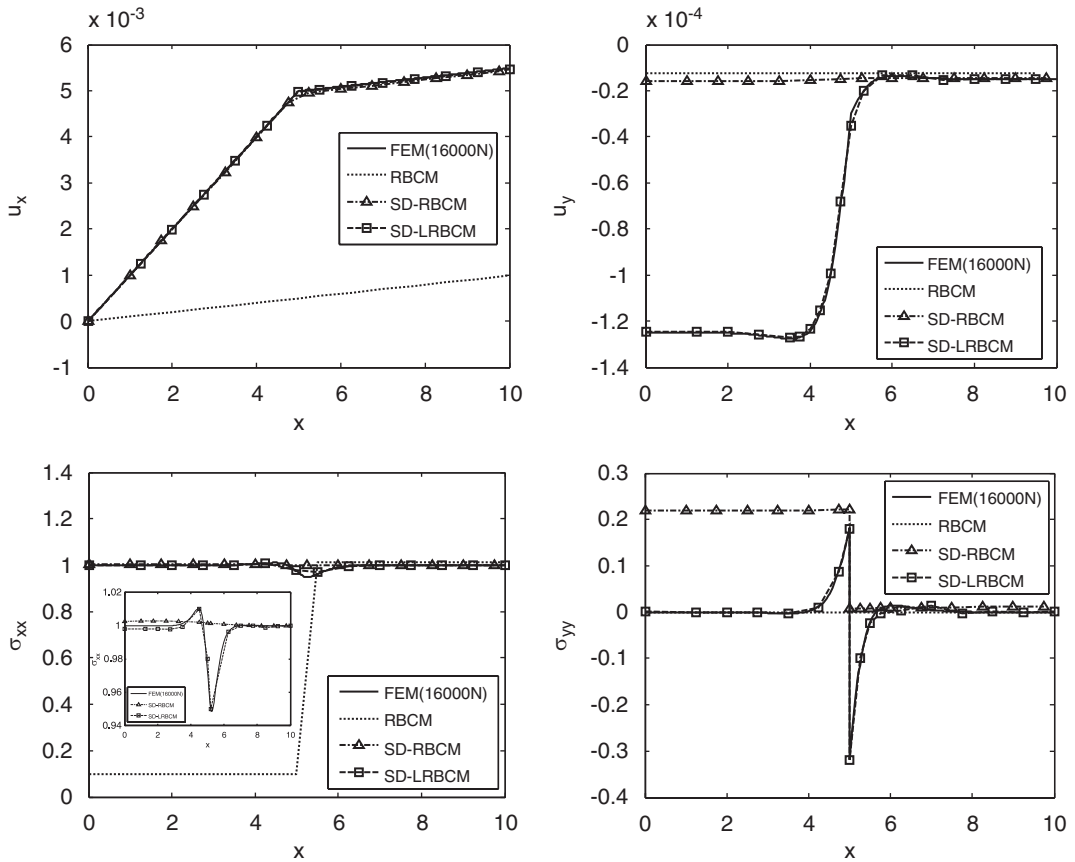

Figure 7. Comparison of displacement and stress solutions obtained by RBCM, SD-RBCM, and SD-LRBCM.

properties are Young's moduli $E^+ = 1.0 \times 10^3$, $E^- = 1.0 \times 10^4$, and the Poisson ratio $v^+ = 0.25$, $v^- = 0.3$. Total of 330 source points and 1320 collocation points are used as shown in Figure 10. Owing to symmetry, only the first quadrant of the plate is modeled. The dimension is 5.0×5.0 and the radius of the circular inclusion is $r = 1.0$. The exact analytical tractions [36] are prescribed on the right and top edges of the quarter model.

Weights for the weighted collocation following (37) are $\sqrt{w_g^+} = \sqrt{w_g^-} = \sqrt{\bar{w}_g} = 10^6$, $\sqrt{w_h^+} = 10$, $\sqrt{w_h^-} = 1$, $\sqrt{\bar{w}_h} = 1$. Figure 11 shows the comparison of displacement and stress solutions along $x = 0$ obtained by RBCM, SD-RBCM, and SD-LRBCM. Results again show that worst results generated by RBCM and best results by SD-LRBCM, although in this problem the SD-RBCM results are already quite good. Convergence in L2- and H1-error norms of the three methods is compared in Figure 12. The two methods with subdomain collocation converge much better than the method with standard collocation. Further, SD-LRBCM converges much faster than SD-RBCM.

DOI: 10.1002/nme

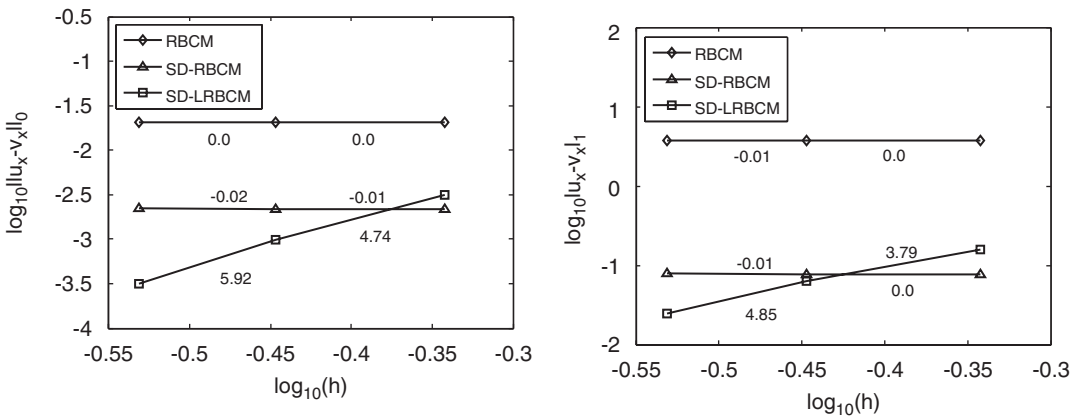

Figure 8. Comparison of L2- and H1-error norms generated by RBCM, SD-RBCM, and SD-LRBCM.

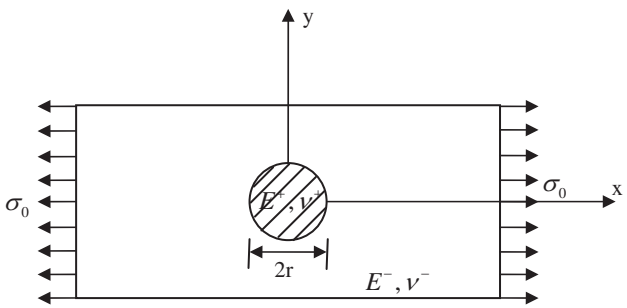

Figure 9. Plate with circular inclusion subjected to horizontal traction.

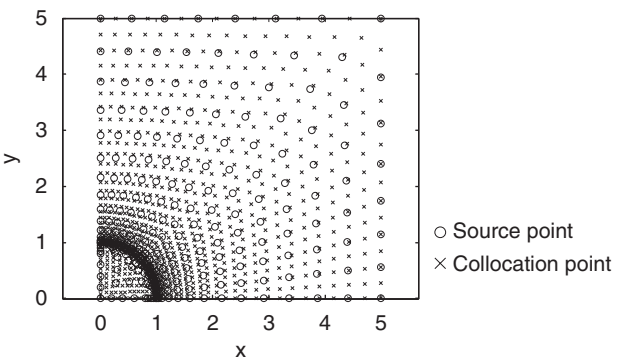

Figure 10. Discretization of the inclusion problem.

DOI: 10.1002/nme

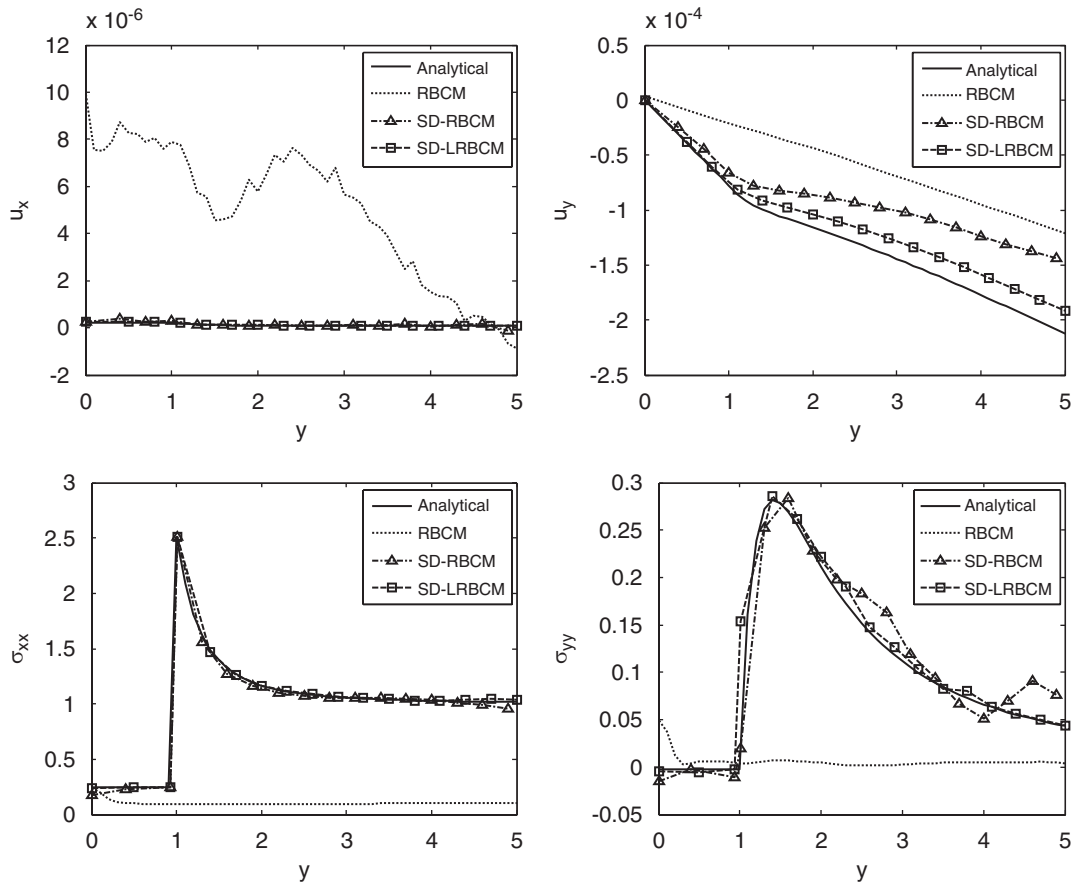

Figure 11. Displacements and stresses along $x = 0$ of the quarter plate obtained by RBCM, SD-RBCM, and SD-LRBCM.

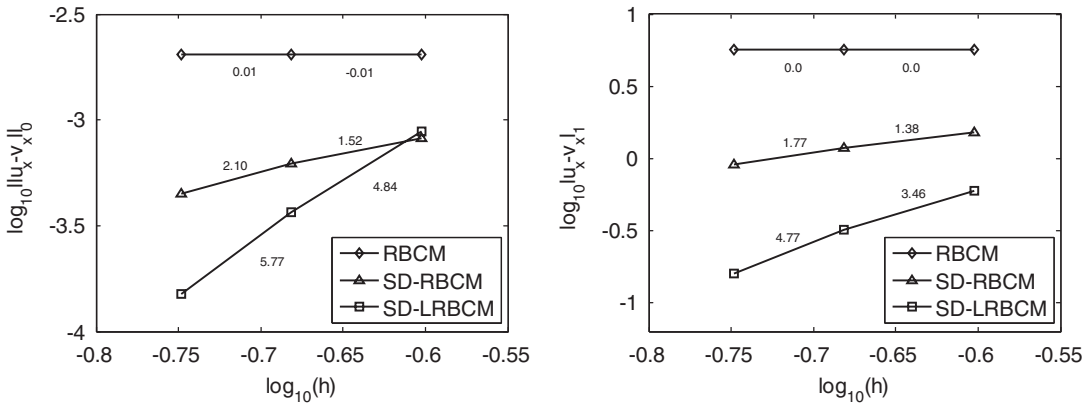

Figure 12. Comparison of L2- and H1-error norms generated by RBCM, SD-RBCM, and SD-LRBCM.

DOI: 10.1002/nme

6. CONCLUSIONS

Solving partial differential equations by radial basis functions (RBFs) in conjunction with strong form collocation has achieved much success in recent years for problems with smooth solution. Nonetheless, little has been done for problem with nonsmooth solution using this approach. Elasticity problem with heterogeneous materials is one typical example of this kind. Unlike weak form approach where the second-order differentiation is reduced to first-order differentiation, strong form collocation encounters the difficulty when discontinuous material properties exist. This yields an awkward situation: either material interface cannot be detected if none of the collocation point is located on the interface, or derivatives of discontinuous material properties at the material interface cannot be properly dealt with.

In this paper, we proposed a subdomain collocation method for solving heterogeneous elasticity. The original heterogeneous problem is first sub-divided into sub-problems where each of the corresponding subdomain has homogeneous material properties. For each sub-problem, the solution is approximated by using only the RBFs with their source points located in the subdomain. Each sub-problem is discretized by strong form collocation, and the collocation equations of all sub-problems with proper interface conditions are then solved simultaneously. Error analysis is also performed for the proposed method, and the results suggest that both displacement continuity and traction equilibrium conditions along the materials interfaces should both be imposed for optimum convergence in the proposed strong form collocation approach. *More specifically*, *if radial basis collocation method* (*RBCM*) *exhibits exponential convergence in homogeneous problem*, *same convergence properties exist in subdomain radial basis collocation method* (*SD-RBCM*) *if the errors on the material interfaces are well controlled*.

Several numerical examples were analyzed to examine the effectiveness of the proposed method. It is shown that the standard RBCM generates significant errors near material interface and in some cases with large errors throughout the whole domain. On the other hand, subdomain collocation method effectively captures derivatives along the material interfaces and provides substantial improvement in the solution compared with the standard collocation method. For problems exhibiting localized behavior near material interfaces, an L-RBFs constructed using RK function as the localizing function of RBF [21] is further introduced in addition to the employment of subdomain collocation. The convergence study demonstrates that the proposed SD-RBCM converges exponentially. Similar convergence is observed when L-RBFs are employed.

APPENDIX A

The explicit expressions of the matrices and vectors in (32)–(33) are defined here.

$$\mathbf{A}_L^+ = \begin{bmatrix} \mathbf{L}^+(\mathbf{\Phi}^{+^{\mathrm{T}}}(\mathbf{p}_1^+)), & \mathbf{0} \\ \vdots & \\ \mathbf{L}^+(\mathbf{\Phi}^{+^{\mathrm{T}}}(\mathbf{p}_{N_p^+}^+)), & \mathbf{0} \end{bmatrix}, \quad \mathbf{A}_L^- = \begin{bmatrix} \mathbf{0}, & \mathbf{L}^-(\mathbf{\Phi}^{-^{\mathrm{T}}}(\mathbf{p}_1^-)) \\ & \vdots \\ \mathbf{0}, & \mathbf{L}^-(\mathbf{\Phi}^{-^{\mathrm{T}}}(\mathbf{p}_{N_p^-}^+)) \end{bmatrix} \tag{A1}$$

DOI: 10.1002/nme

$$\mathbf{A}_g^+ = \begin{bmatrix} \mathbf{B}_g^+(\mathbf{\Phi}^{+\mathrm{T}}(\mathbf{q}_1^+)), & \mathbf{0} \\ \vdots & \\ \mathbf{B}_g^+(\mathbf{\Phi}^{+\mathrm{T}}(\mathbf{q}_{N_q^+}^+)), & \mathbf{0} \end{bmatrix}, \quad \mathbf{A}_g^- = \begin{bmatrix} \mathbf{0}, & \mathbf{B}_g^-(\mathbf{\Phi}^{-\mathrm{T}}(\mathbf{q}_1^-)) \\ & \vdots \\ \mathbf{0}, & \mathbf{B}_g^-(\mathbf{\Phi}^{-\mathrm{T}}(\mathbf{q}_{N_q^-}^-)) \end{bmatrix} \tag{A2}$$

$$\mathbf{A}_h^+ = \begin{bmatrix} \mathbf{B}_h^+(\mathbf{\Phi}^{+\mathrm{T}}(\mathbf{r}_1^+)), & \mathbf{0} \\ \vdots & \\ \mathbf{B}_h^+(\mathbf{\Phi}^{+\mathrm{T}}(\mathbf{r}_{N_r^+}^+)), & \mathbf{0} \end{bmatrix}, \quad \mathbf{A}_h^+ = \begin{bmatrix} \mathbf{0}, & \mathbf{B}_h^-(\mathbf{\Phi}^{-\mathrm{T}}(\mathbf{r}_1^-)) \\ & \vdots \\ \mathbf{0}, & \mathbf{B}_h^-(\mathbf{\Phi}^{-\mathrm{T}}(\mathbf{r}_{N_r^-}^-)) \end{bmatrix} \tag{A3}$$

$$\mathbf{\Lambda}_g = \begin{bmatrix} \mathbf{\Phi}^{+\mathrm{T}}(\mathbf{t}_1), & -\mathbf{\Phi}^{-\mathrm{T}}(\mathbf{t}_1) \\ \vdots & \vdots \\ \mathbf{\Phi}^{+\mathrm{T}}(\mathbf{t}_{N_t}), & -\mathbf{\Phi}^{-\mathrm{T}}(\mathbf{t}_{N_t}) \end{bmatrix} \tag{A4}$$

$$\mathbf{\Lambda}_h = \begin{bmatrix} \mathbf{B}_h^+\mathbf{\Phi}^{+\mathrm{T}}(\mathbf{t}_1), & \mathbf{B}_h^-\mathbf{\Phi}^{-\mathrm{T}}(\mathbf{t}_1) \\ \vdots & \vdots \\ \mathbf{B}_h^+\mathbf{\Phi}^{+\mathrm{T}}(\mathbf{t}_{N_t}), & \mathbf{B}_h^-\mathbf{\Phi}^{-\mathrm{T}}(\mathbf{t}_{N_t}) \end{bmatrix} \tag{A5}$$

$$\mathbf{b}_L^+ = \begin{bmatrix} \mathbf{f}(\mathbf{p}_1^+) \\ \vdots \\ \mathbf{f}(\mathbf{p}_{N_p^+}^+) \end{bmatrix}, \quad \mathbf{b}_L^- = \begin{bmatrix} \mathbf{f}(\mathbf{p}_1^-) \\ \vdots \\ \mathbf{f}(\mathbf{p}_{N_p^-}^-) \end{bmatrix} \tag{A6}$$

$$\mathbf{b}_g^+ = \begin{bmatrix} \mathbf{g}(\mathbf{q}_1^+) \\ \vdots \\ \mathbf{g}(\mathbf{q}_{N_q^+}^+) \end{bmatrix}, \quad \mathbf{b}_g^- = \begin{bmatrix} \mathbf{g}(\mathbf{q}_1^-) \\ \vdots \\ \mathbf{g}(\mathbf{q}_{N_q^-}^-) \end{bmatrix} \tag{A7}$$

$$\mathbf{b}_h^+ = \begin{bmatrix} \mathbf{h}(\mathbf{r}_1^+) \\ \vdots \\ \mathbf{h}(\mathbf{r}_{N_r^+}^+) \end{bmatrix}, \quad \mathbf{b}_h^- = \begin{bmatrix} \mathbf{h}(\mathbf{r}_1^-) \\ \vdots \\ \mathbf{h}(\mathbf{r}_{N_r^-}^-) \end{bmatrix} \tag{A8}$$

ACKNOWLEDGEMENTS

The support of this work by Lawrence Livermore National Laboratory (U.S.A.) to the first and fourth authors, the support by National Natural Science Foundation of China (NSFC) under Project No. 10572104

DOI: 10.1002/nme

to the second author, and the support by National Science Council of Taiwan, R. O. C., under project number NSC 96-2115-M-029-002-MY2 to the third author are greatly acknowledged.

REFERENCES

1. Belytschko T, Lu YY, Gu L. Element-free Galerkin methods. *International Journal for Numerical Methods in Engineering* 1994; **37**:229–256.
2. Liu WK, Jun S, Zhang YF. Reproducing kernel particle methods. *International Journal for Numerical Methods in Fluids* 1995; **20**:1081–1106.
3. Duarte CA, Oden JT. An h-p adaptive method using clouds. *Computer Methods in Applied Mechanics and Engineering* 1996; **139**:237–262.
4. Babuska I, Melenk JM. The partition of unity method. *International Journal for Numerical Methods in Engineering* 1997; **40**:727–758.
5. Chen JS, Pan C, Wu CT, Liu WK. Reproducing kernel particle methods for large deformation analysis of nonlinear structures. *Computer Methods in Applied Mechanics and Engineering* 1996; **139**:195–227.
6. Atluri SN, Zhu TL. The meshless local Petrov–Galerkin (MLPG) approach for solving problems in elasto-statics. *Computational Mechanics* 2000; **25**:169–179.
7. Kansa EJ. Multiquadrics—a scattered data approximation scheme with applications to computational fluid-dynamics: I. Surface approximations and partial derivatives estimates. *Computers and Mathematics with Applications* 1992; **19**:127–145.
8. Fasshauer GE. Solving differential equations with radial basis functions: multilevel methods and smoothing. *Advances in Computational Mathematics* 1999; **11**:139–159.
9. Franke R, Schaback R. Solving partial differential equations by collocation using radial functions. *Applied Mathematics and Computation* 1998; **93**:73–82.
10. Hu HY, Li ZC, Cheng AHD. Radial basis collocation method for elliptic equations. *Computers and Mathematics with Applications* 2005; **50**:289–320.
11. Onate E, Idelsohn S, Zienkiewicz OC, Taylor RL. A finite point method in computational mechanics: application to convective transport and fluid flow. *International Journal for Numerical Methods in Engineering* 1996; **39**:3839–3866.
12. Kansa EJ. Multiquadrics—a scattered data approximation scheme with applications to computational fluid-dynamics: II. Solutions to parabolic, hyperbolic and elliptic partial differential equations. *Computers and Mathematics with Applications* 1992; **19**:147–161.
13. Schaback R, Wendland H. Using compactly supported radial basis functions to solve partial differential equations. *Boundary Element Technology* 1999; **XIII**:311–324.
14. Wendland H. Piecewise polynomial, positive definite and compactly supported radial functions of minimal degree. *Advances in Computational Mathematics* 1995; **4**:389–396.
15. Wendland H. Error estimates for interpolation by compactly supported radial basis functions of minimal degree. *Journal of Approximation Theory* 1998; **93**:258–272.
16. Xiao JR, McCarthy MA. A local heaviside weighted meshless method for two-dimensional solids using radial basis function. *Computational Mechanics* 2003; **31**:301–315.
17. Wang JG, Liu GR. Point interpolation meshless method based on radial basis functions. *International Journal for Numerical Methods in Engineering* 2002; **54**:1623–1648.
18. Chen JS, Wang HP. New boundary condition treatments in meshless computation of contact problems. *Computer Methods in Applied Mechanics and Engineering* 2000; **187**:441–468.
19. Liu GR, Gu YT. A local radial point interpolation method (LRPIM) for free vibration analyses of 2-D solids. *Journal of Sound and Vibration* 2001; **246**:29–46.
20. Shu C, Ding H, Yeo KS. Local radial basis function-based differential quadrature method and its application to solve two-dimensional incompressible Navier–Stokes equations. *Computer Methods in Applied Mechanics and Engineering* 2003; **192**:941–954.
21. Chen JS, Hu W, Hu HY. Reproducing kernel enhanced local radial basis collocation method. *International Journal for Numerical Methods in Engineering* 2008; **75**:600–627.
22. Wong SM, Hon YC, Li TS, Chung SL, Kansa EJ. Multizone decomposition for simulation of time-dependent problems using the multiquadric scheme. *Computers and Mathematics with Applications* 1999; **37**:23–43.

DOI: 10.1002/nme

23. Kansa EJ, Hon YC. Circumventing the ill-conditioning problem with multiquadric radial basis functions: applications to elliptic partial differential equations. *Computers and Mathematics with Applications* 2000; **4**: 123–137.
24. Ling L, Opfer R, Schaback R. Results on meshless collocation techniques. *Engineering Analysis with Boundary Elements* 2006; **30**:247–253.
25. Cordes LW, Moran B. Treatment of material discontinuity in the element-free Galerkin method. *Computer Methods in Applied Mechanics and Engineering* 1996; **139**:75–89.
26. Wang D, Chen JS, Sun L. Homogenization of magnetostrictive particle-filled elastomers using an interface-enriched reproducing kernel particle method. *Journal of Finite Element Analysis and Design* 2003; **39**(8):765–782.
27. Masuda S, Noguchi H. Analysis of structure with material interface by meshfree method. *Computer Modeling in Engineering and Science* 2006; **11**(3):131–144.
28. Hardy RL. Multiquadric equations of topography and other irregular surfaces. *Journal of Geophysical Research* 1971; **176**:1905–1915.
29. Madych WR, Nelson SA. Bounds on multivariate polynomials and exponential error estimates for multiquadric interpolation. *Journal of Approximation Theory* 1992; **70**:94–114.
30. Lancaster P, Salkauskas K. Surfaces generated by moving least squares methods. *Mathematics of Computation* 1981; **37**:141–158.
31. Hu HY, Chen JS, Hu W. Weighted radial basis collocation method for boundary value problems. *International Journal for Numerical Methods in Engineering* 2001; **69**:2736–2757.
32. Quarteroni A, Valli A. *Numerical Approximation of Partial Differential Equations*. Springer: Berlin, Heidelberg, 1994.
33. Hu HY, Li ZC. Collocation methods for Poisson's equation. *Computer Methods in Applied Mechanics and Engineering* 2006; **195**:4139–4160.
34. Strang G, Fix GJ. *Analysis of the Finite Element Method*. Prentice-Hall: Englewood Cliffs, NJ, 1973.
35. Hu HY, Li ZC. Combinations of collocation and finite element methods for Poisson's equation. *Computers and Mathematics with Applications* 2006; **51**:1831–1853.
36. Atkin RJ, Fox N. *An Introduction to the Theory of Elasticity*. Longman: London, 1980.

DOI: 10.1002/nme